Contemporary Mathematics
https://ojs.wiserpub.com/index.php/CM/

Research Article

Optimal Control Strategies for Dual-Strain Hepatitis B Dynamics: A Mathematical and Cost-Effectiveness Study

Moustafa El-Shahed*, **Reem Alharbi**

Department of Mathematics, College of Science, Qassim University, P.O. Box 6644, Buraydah 51452, Saudi Arabia
E-mail: m.elshahed@qu.edu.sa

Received: 01 July 2025; **Revised:** 12 August 2025; **Accepted:** 14 August 2025

Abstract: This study presents a mathematical model to describe the transmission dynamics of the Hepatitis B Virus (HBV), accounting for two distinct viral strains. The basic reproduction number, R_0, is derived using the next-generation matrix method, and three equilibrium points are identified. Stability analysis reveals that the disease-free equilibrium is locally asymptotically stable when $R_0 < 1$, the first strain-free equilibrium is stable when $R_{02} > R_{01}$, and the endemic equilibrium is stable when $R_0 > 1$. An optimal control problem is then formulated to evaluate the effectiveness of two intervention strategies: vaccination and treatment. The objective is to minimize infection levels and reduce economic burden. Using Pontryagin's Maximum Principle, the necessary conditions for optimal control are established within a deterministic framework. Numerical simulations, implemented in MATLAB, support the theoretical findings and demonstrate the impact of the proposed controls. Cost-effectiveness analysis indicates that treatment is the most economically efficient strategy. The model offers practical insights for HBV-endemic regions, particularly those with constrained healthcare resources.

Keywords: Hepatitis B Virus (HBV), multi-strain model stability, optimal control, cost-effectiveness analysis

MSC: 92D30, 49K15, 93C15

1. Introduction

The liver is one of the most vital organs in the human body, playing a crucial role in metabolism, detoxification, and various other functions. Liver infections can lead to a range of diseases, one of the most notable being Hepatitis B Virus (HBV). HBV is a contagious disease that causes inflammation of the liver. The virus itself does not directly damage liver cells; instead, the immune system's response to the infection leads to liver inflammation [1, 2]. It has been demonstrated that chronic infection with HBV is a significant contributor to the development of liver cancer due to both the direct and indirect effects of the virus on liver cells over time [3]. Recent global estimates indicate that approximately 254 million individuals were living with chronic HBV infection in 2022, with around 1.2 million new HBV infections occurring that year alone [4]. Alarmingly, only 13% of those infected were aware of their status, and merely 3% were receiving treatment [5].

DOI: https://doi.org/10.37256/cm.6520257666

In the United States, approximately 640,000 adults were living with chronic HBV as of 2022, with nearly half of them undiagnosed [6]. The age-adjusted HBV-related mortality rate remained at 0.44 deaths per 100,000 population in 2023, which still exceeds the national target of 0.37 [7].

Currently, mathematical modeling is a powerful tool used to describe the dynamic behavior of various diseases [8–14]. Mathematical models have played an important and fundamental role in the epidemiology of the HBV by enhancing our understanding of the key factors that lead to the spread and progression of this disease. In numerous previous studies on mathematical models of the HBV, the primary focus has been on exploring strategies to control its spread, including treatment, vaccination, and public health interventions. These models have provided valuable insights and data on the impact of vaccination and treatment as control strategies for HBV [15–33].

Optimal control theory plays a crucial role in infectious disease modeling as it provides a systematic framework for identifying the most effective intervention strategies that minimize disease burden and intervention costs over time. By incorporating time-dependent control variables–such as vaccination, treatment, and public health campaigns–into mathematical models, optimal control helps policymakers evaluate the trade-offs between health outcomes and resource allocation. This approach supports evidence-based decision-making, particularly in settings where resources are limited and disease dynamics are complex [34–36]. Zhang [37] formulated a mathematical model that incorporates vaccination and treatment to study the transmission dynamics of HBV in China, highlighting the potential effectiveness of these control measures in reducing HBV prevalence. Recently, Khan et al. discussed epidemiological models of hepatitis B dynamics by incorporating a variety of influencing parameters [22, 38–40].

In [40], the authors developed a mathematical model for HBV incorporating a nonlinear transmission rate. Through numerical simulations, they assessed the practicality and impact of a proposed control strategy. Their findings indicated that sustained implementation of this strategy could potentially lead to the complete eradication of HBV from the population.

Clinical and virological studies have reported the coexistence of multiple HBV genotypes or strains within specific populations, which may exhibit different transmission dynamics, levels of virulence, and responses to treatment. Ignoring this heterogeneity may lead to oversimplified predictions and suboptimal control strategies. Furthermore, modeling two distinct strains allows for capturing competitive interactions between strains, investigating possible strain replacement, and assessing the effectiveness of interventions under heterogeneous infection pressures [41–43].

Although various models have been formulated to analyze the spread and behavior of HBV, most existing studies focus on a single-strain framework and often assume homogeneous transmission or neglect important intervention aspects. These limitations reduce the ability of such models to reflect the real-world complexity of HBV epidemiology, especially in regions where multiple strains co-circulate and interact competitively. Moreover, many of these models lack the integration of optimal control theory and economic evaluation, which are essential for guiding public health decision-making in resource-limited settings.

This study addresses these gaps by formulating a two-strain HBV transmission model that captures strain-specific interactions and outcomes. In addition, we incorporate a nonlinear optimal control framework involving vaccination and treatment strategies, and we assess the relative efficiency of these interventions through cost-effectiveness analysis. Thus, the proposed approach not only advances the theoretical modeling of HBV but also provides practical insights to support efficient and economically viable control policies. In this paper, we develop a two-strain HBV epidemic model, building on the foundational works [44–49]. The work is structured into six main sections. In Section 1, the system is formulated as a set of six differential equations that describe the transmission dynamics of the disease within the population. The positivity and boundedness of the solutions are also established to ensure the mathematical validity of the model. Section 2 focuses on analyzing the model by calculating the equilibrium points, determining the basic reproduction number R_0, and analyzing the local and global stability of these points. Section 4 presents a bifurcation analysis. In Section 5, an optimal control strategy is incorporated into the model to minimize disease transmission by applying control theory techniques. Section 6 is devoted to the sensitivity analysis to identify the most influential parameters on R_0 and the overall behavior of the system. Finally, Section 7 presents numerical simulations that validate and illustrate the theoretical findings.

2. Mathematical formulation

In this study, we formulate a mathematical model to enhance the understanding of HBV transmission dynamics. The model incorporates two distinct viral strains and is constructed based on previous studies [44–49], under the following assumptions:

• The total population is divided into six mutually exclusive compartments: susceptible, acute and chronic infections for each of the two HBV strains, and recovered individuals.

• Susceptible individuals can become infected with either strain of HBV through contact with infectious individuals.

• Acutely infected individuals may either recover with permanent immunity or progress to the chronic stage.

• Individuals infected with one strain do not acquire cross-immunity against the other strain.

• Recovered individuals are assumed to have long-term immunity to both strains and do not return to susceptibility.

• The disease-induced mortality is assumed to occur only in the chronic compartments.

The model is structured into six epidemiological compartments, defined as follows:

• S: Susceptible individuals who are at risk of HBV infection.

• A_1: Individuals acutely infected with strain 1 of HBV.

• C_1: Individuals chronically infected with strain 1 of HBV.

• A_2: Individuals acutely infected with strain 2 of HBV.

• C_2: Individuals chronically infected with strain 2 of HBV.

• R: Recovered individuals with long-term immunity to both strains.

The dynamics of these compartments are described below.

$$\begin{aligned}
\frac{dS}{dt} &= \Lambda - \beta_1 S(A_1 + \rho_1 C_1) - \beta_2 S(A_2 + \rho_2 C_2) - (\nu + \mu_1)S, \\
\frac{dA_1}{dt} &= \beta_1 S(A_1 + \rho_1 C_1) - (\gamma_1 + \mu_1 + \theta_1)A_1 - \omega A_1, \\
\frac{dC_1}{dt} &= \theta_1 A_1 - (\gamma_2 + \mu_1 + \mu_2)C_1, \\
\frac{dA_2}{dt} &= \beta_2 S(A_2 + \rho_2 C_2) - (\gamma_3 + \mu_1 + \theta_2)A_2 + \omega A_1, \\
\frac{dC_2}{dt} &= \theta_2 A_2 - (\gamma_4 + \mu_1 + \mu_3)C_2, \\
\frac{dR}{dt} &= \gamma_1 A_1 + \gamma_2 C_1 + \gamma_3 A_2 + \gamma_4 C_2 + \nu S - \mu_1 R.
\end{aligned} \tag{1}$$

We define Λ as the birth rate and ν as the vaccination rate. The parameter β_1 represents the transmission rate of acute hepatitis B of the first strain, and ρ_1 represents the relative infectiousness of individuals with acute infection compared to those with chronic infection for the first strain. In contrast, $\beta_1.\rho_1$ denotes the rate of transmission of chronic infections of the first strain. Similarly, β_2 represents the transmission rate of acute hepatitis B of the second strain, ρ_2 represents the relative infectiousness of individuals with acute infection compared to those with chronic infection for the second strain, and $\beta_2.\rho_2$ corresponds to the transmission rate of chronic infection of the second strain. The parameter ω represents the mutation rate from the first strain to the second strain. The natural mortality rate for all compartments is denoted by μ_1, while μ_2 accounts for the additional mortality caused by chronic infection of the first strain, which exceeds the

natural death rate. Likewise, μ_3 represents the additional mortality due to the chronic infection of the second strain. The parameters θ_1 and θ_2 represent the progression from acute to chronic HBV infection for the first and second strains, respectively. Recovery rates are defined as follows: γ_1 for acute infection of the first strain, γ_2 for chronic infection of the first strain, γ_3 for acute infection of the second strain, and γ_4 for chronic infection of the second strain. Figure 1 provides a flowchart illustrating the compartmental structure of the HBV model.

For simplicity, we assume that:

$$q_1 = \nu + \mu_1,\ q_2 = \gamma_1 + \mu_1 + \theta_1,\ q_3 = \gamma_2 + \mu_1 + \mu_2,\ q_4 = \gamma_3 + \mu_1 + \theta_2,\ q_5 = \gamma_4 + \mu_1 + \mu_3. \tag{2}$$

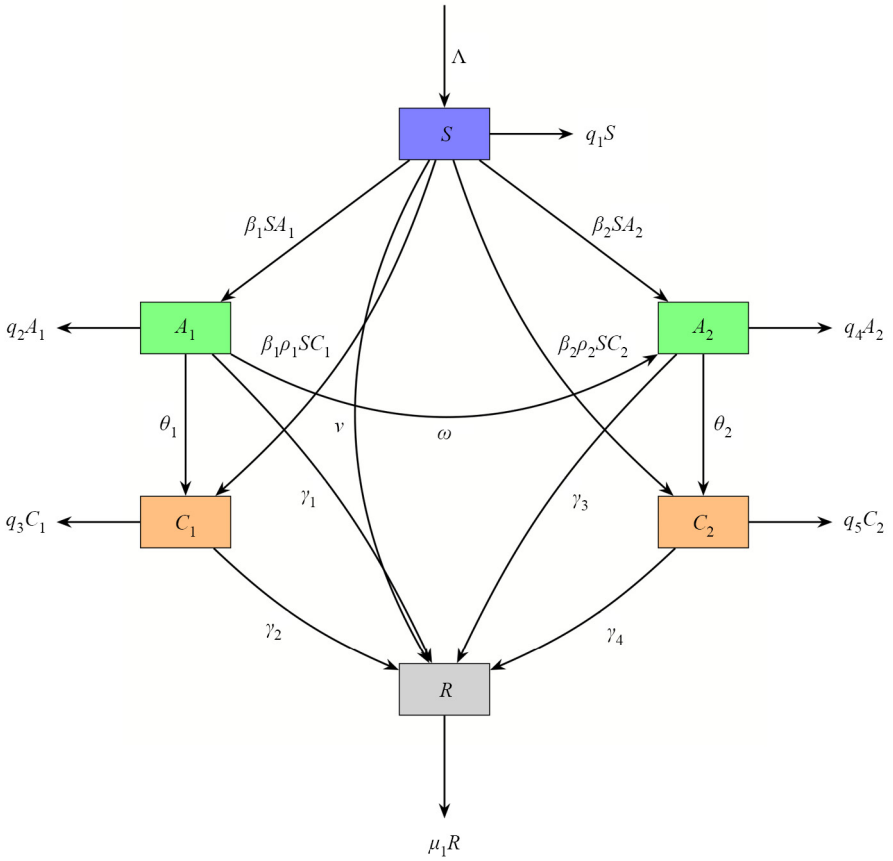

Figure 1. Flowchart illustrating the structure of the HBV model

3. Positivity and boundedness

We aim to prove that all solutions of system (1) with nonnegative initial conditions are biologically feasible. Specifically, if the initial conditions are nonnegative, then the corresponding solutions remain nonnegative for all $t \geq 0$. In addition, we will demonstrate that the solutions remain bounded over time.

Theorem 1 For non-negative initial conditions, every solution of the system (1) remains positive.

Proof. The first equation of the HBV system (1) yields

$$\frac{dS}{dt} = \Lambda - S\Lambda_0, \tag{3}$$

where $\Lambda_0 = \beta_1(A_1 + \rho_1 C_1) + \beta_2(A_2 + \rho_2 C_2) + q_1$. Applying the initial condition, it follows that:

$$S \geq S(0)\exp(-\Lambda_0 t).$$

Similarly, we obtain the rest

$$A_1(t) \geq A_1(0)\exp[-(q_2+\omega)t], \quad C_1(t) \geq C_1(0)\exp(-q_3 t), \tag{4}$$

$$A_2(t) \geq A_2(0)\exp(-q_4 t), \quad C_2(t) \geq C_2(0)\exp(-q_5 t), \quad R(t) \geq R(0)\exp(-\mu_1 t). \tag{5}$$

Thus, the solution of the system (1) remains positive. □

Theorem 2 The solutions of HBV system (1) in $\mathbb{R}^6_+$ are uniformly bounded.

Proof. Let $N(t)$ represent the total population in all epidemiological compartments such that:

$$N = S + A_1 + C_1 + A_2 + C_2 + R. \tag{6}$$

By substituting the temporal derivatives into and incorporating the values of system (1), the following expression can be derived:

$$\frac{dN}{dt} + \mu_1 N = \Lambda - \mu_2 C_1 - \mu_3 C_2. \tag{7}$$

Since $\mu_2,\ \mu_3,\ C_1,\ C_2$ are positive parameters we get:

$$\frac{dN}{dt} + \mu_1 N \leq \Lambda. \tag{8}$$

The solution to this differential equation yields the following result

$$0 < N(t) \leq \frac{\Lambda}{\mu_1} + \left[N(0) - \frac{\Lambda}{\mu_1}\right]\exp(-\mu_1 t). \tag{9}$$

As $t \to \infty$, it follows that $0 < N(t) \leq \frac{\Lambda}{\mu_1}$. □

4. Model analysis

In this Section, we will investigate the qualitative analysis of the HBV system.

4.1 *Equilibrium points*

The equilibrium points of the HBV model described by system (1) are given below:

$$\begin{aligned} E_0 &= (S_0^*,\ 0,\ 0,\ 0,\ 0,\ R_0^*), \\ E_1 &= (S^*,\ 0,\ 0,\ A_2^*,\ C_2^*,\ R^*), \\ E_2 &= (S^{**},\ A_1^{**},\ C_1^{**},\ A_2^{**},\ C_2^{**},\ R^{**}), \end{aligned} \tag{10}$$

where

$$S_0^* = \frac{\Lambda}{q_1}, \quad R_0^* = \frac{\nu\Lambda}{\mu_1 q_1}, \quad S^* = \frac{q_4 q_5}{q_5\beta_2 + \beta_2\theta_2\rho_2}, \quad A_2^* = \frac{\Lambda}{q_4} - \frac{q_1 q_5}{q_5\beta_2 + \beta_2\theta_2\rho_2}, \tag{11}$$

$$C_2^* = \frac{\theta_2\Lambda}{q_4 q_5} - \frac{q_1\theta_2}{q_5\beta_2 + \beta_2\theta_2\rho_2}, \quad R^* = \frac{1}{\mu_1}[\nu S^* + \gamma_3 A_2^* + \gamma_4 C_2^*], \tag{12}$$

$$S^{**} = \frac{q_3(q_2+\omega)}{\beta_1(q_3+\theta_1\rho_1)}, \ A_1^{**} = \frac{A_2^{**}}{\omega}[q_4 - \frac{\beta_2 S^{**}\rho_2\theta_2}{q_5} - \beta_2 S^{**}], \ C_1^{**} = \frac{\theta_1 A_1^{**}}{q_3}, \tag{13}$$

$$A_2^{**} = \frac{q_5\omega\left(\beta_1\Lambda(q_3+\theta_1\rho_1) - q_1 q_3(q_2+\omega)\right)}{\left(q_3 q_4 q_5\beta_1 + q_4 q_5\beta_1\theta_1\rho_1 - q_2 q_3\beta_2(q_5+\theta_2\rho_2)\right)(q_2+\omega)}, \tag{14}$$

$$C_2^{**} = \frac{\theta_2 A_2^{**}}{q_4}, \ R^{**} = \frac{1}{\mu_1}[\nu S^{**} + \gamma_1 A_1^{**} + \gamma_2 C_1^{**} + \gamma_3 A_2^{**} + \gamma_4 C^{**}]. \tag{15}$$

4.2 *Basic reproduction number*

The basic reproduction number R_0 is a critical parameter in epidemiological modeling. The average number of secondary infections caused by a single infected person in an exposed population, and using the next-generation matrix method [50]. We calculate it by focusing on the equations in system (1) which describe the dynamics of the infected compartments. Let $\mathscr{F}$ represent the rate at which new infections are introduced into the system, and let $\mathscr{V}$ denote the net rate of change within the infected compartments, incorporating both the inflow and outflow due to transitions such as progression, recovery, or removal.

$$\mathscr{F} = \begin{pmatrix} \beta_1 S(A_1 + \rho_1 C_1) \\ \beta_2 S(A_2 + \rho_2 C_2) \\ 0 \\ 0 \end{pmatrix}, \quad \mathscr{V} = \begin{pmatrix} A_1(q_2+\omega) \\ q_4 A_2 - \omega A_1 \\ q_3 C1 - \theta_1 A_1 \\ q_5 C_2 - \theta_2 A_2 \end{pmatrix}. \tag{16}$$

We then construct the Jacobian matrices of $\mathscr{F}$ and $\mathscr{V}$, evaluated at the Disease-Free Equilibrium (DFE), denoted as E_0. These matrices are denoted by $\mathbb{F}$ and $\mathbb{V}$.

$$\mathbb{F} = \begin{bmatrix} \frac{\beta_1 \Lambda}{q_1} & 0 & \frac{\beta_1 \rho_1 \Lambda}{q_1} & 0 \\ 0 & \frac{\beta_1 \Lambda}{q_1} & 0 & \frac{\beta_2 \rho_2 \Lambda}{q_1} \\ 0 & 0 & 0 & 0 \\ 0 & 0 & 0 & 0 \end{bmatrix}, \quad \mathbb{V} = \begin{bmatrix} q_2 + \omega & 0 & 0 & 0 \\ -\omega & q_4 & 0 & 0 \\ -\theta_1 & 0 & q_3 & 0 \\ 0 & -\theta_2 & 0 & q_5 \end{bmatrix}. \tag{17}$$

The basic reproduction number R_0 for the HBV system (1) is defined as the spectral radius of the matrix product $\mathbb{F}\mathbb{V}^{-1}$. It is given by:

$$R_0 = \max\{R_{01}, R_{02}\}, \tag{18}$$

where

$$R_{01} = \frac{\Lambda \beta_1 (q_3 + \theta_1 \rho_1)}{q_1 (q_2 + \omega) q_3}, \; R_{02} = \frac{\Lambda \beta_2 (q_5 + \theta_2 \rho_2)}{q_1 q_4 q_5}. \tag{19}$$

The quantities R_{01} and R_{02} represent the transmission contributions of the first and second HBV strains, respectively. The overall reproduction number R_0 is taken as the maximum of the two, reflecting the dominant transmission potential in the system.

4.3 *Stability of the HBV system*

4.3.1 *Local stability*

In this subsection, we analyze the local asymptotic stability (LAS) of the HBV model.

Theorem 3 The HBV-free equilibrium point E_0 of the system (1) is LAS if $R_0 < 1$.

Proof. At HBV-free equilibrium point E_0 the Jacobian matrix of the HBV system (1) is

$$J(E_0) = \begin{bmatrix} -q_1 & -\frac{\beta_1 \Lambda}{q_1} & -\frac{\beta_1 \Lambda \rho_1}{q_1} & -\frac{\beta_2 \Lambda}{q_1} & -\frac{\beta_2 \Lambda \rho_2}{q_1} & 0 \\ 0 & -q_2 + \frac{\beta_1 \Lambda}{q_1} - \omega & \frac{\beta_1 \Lambda \rho_1}{q_1} & 0 & 0 & 0 \\ 0 & \theta_1 & -q_3 & 0 & 0 & 0 \\ 0 & \omega & 0 & \frac{\beta_2 \Lambda}{q_1} - q_4 & \frac{\beta_2 \Lambda \rho_2}{q_1} & 0 \\ 0 & 0 & 0 & \theta_2 & -q_5 & 0 \\ \nu & \gamma_1 & \gamma_2 & \gamma_3 & \gamma_4 & -\mu_1 \end{bmatrix}. \tag{20}$$

The characteristic polynomial corresponding to $J(E_0)$ is expressed as:

$$\begin{vmatrix} -q_1-\lambda & -\frac{\beta_1\Lambda}{q_1} & -\frac{\beta_1\Lambda\rho_1}{q_1} & -\frac{\beta_2\Lambda}{q_1} & -\frac{\beta_2\Lambda\rho_2}{q_1} & 0 \\ 0 & -\omega-q_2+\frac{\Lambda\beta_1}{q_1}-\lambda & \frac{\beta_1\Lambda\rho_1}{q_1} & 0 & 0 & 0 \\ 0 & \theta_1 & -q_3-\lambda & 0 & 0 & 0 \\ 0 & \omega & 0 & \frac{\Lambda\beta_2}{q_1}-q_4-\lambda & \frac{\beta_2\Lambda\rho_2}{q_1} & 0 \\ 0 & 0 & 0 & \theta_2 & -q_5-\lambda & 0 \\ \nu & \gamma_1 & \gamma_2 & \gamma_3 & \gamma_4 & -\mu_1-\lambda \end{vmatrix} = 0. \tag{21}$$

This determinant simplifies to:

$$(\lambda+q_1)(-\lambda-\mu_1)\begin{vmatrix} -\lambda-\omega-q_2+\frac{\Lambda\beta_1}{q_1} & \frac{\beta_1\Lambda\rho_1}{q_1} & 0 & 0 \\ \theta_1 & -\lambda-q_3 & 0 & 0 \\ \omega & 0 & -\lambda-q_4+\frac{\Lambda\beta_2}{q_1} & \frac{\beta_2\Lambda\rho_2}{q_1} \\ 0 & 0 & \theta_2 & -\lambda-q_5 \end{vmatrix} = 0. \tag{22}$$

The characteristic equation yields six eigenvalues. Among them, the first two are $\lambda_1=-\mu_1$ and $\lambda_2=-q_1$, which are clearly negative. The remaining four eigenvalues are determined from two quadratic factors derived from the determinant.

$$\left[\lambda^2+\lambda\left(q_4+q_5-\frac{\Lambda\beta_2}{q_1}\right)+q_4q_5(1-R_{02})\right]\cdot\left[\lambda^2+\left(q_2+\omega+q_3-\frac{\Lambda\beta_1}{q_1}\right)\lambda+q_3(q_2+\omega)(1-R_{01})\right]=0. \tag{23}$$

The first quadratic has negative roots provided that:

$$q_4+q_5-\frac{\Lambda\beta_2}{q_1}>0 \quad \text{and} \quad R_{02}<1. \tag{24}$$

Note that the condition $R_{02}<1$ inherently implies:

$$q_4 + q_5 - \frac{\Lambda\beta_2}{q_1} > 0, \tag{25}$$

as shown below:

$$\begin{aligned} R_{02} < 1 \Rightarrow \frac{\beta_2\Lambda(q_5+\theta_2\rho_2)}{q_1q_4q_5} < 1 \Rightarrow \Lambda\beta_2q_5 + \Lambda\beta_2\theta_2\rho_2 < q_1q_4q_5 \Rightarrow \Lambda\beta_2(q_5+\theta_2\rho_2) < q_1q_4q_5 \\ \Rightarrow \Lambda\beta_2 < q_1q_4 \Rightarrow \frac{\Lambda\beta_2}{q_1} < q_4 \Rightarrow q_4 + q_5 - \frac{\Lambda\beta_2}{q_1} > 0. \end{aligned} \tag{26}$$

Similarly, the second quadratic:

$$\lambda^2 + \left(q_2 + \omega + q_3 - \frac{\Lambda\beta_1}{q_1}\right)\lambda + q_3(q_2+\omega)(1-R_{01}) = 0, \tag{27}$$

which has negative roots provided that:

$$q_2 + \omega + q_3 - \frac{\Lambda\beta_1}{q_1} > 0 \quad \text{and} \quad R_{01} < 1. \tag{28}$$

Note that the condition $R_{01} < 1$ inherently implies:

$$q_2 + \omega + q_3 - \frac{\Lambda\beta_1}{q_1} > 0, \tag{29}$$

as shown below:

$$R_{01} < 1 \Rightarrow \frac{\Lambda\beta_1(q_3+\theta_1\rho_1)}{q_1(q_2+\omega)q_3} < 1 \Rightarrow \Lambda\beta_1(q_3+\theta_1\rho_1) < q_1(q_2+\omega)q_3 \Rightarrow \Lambda\beta_1 < q_1(q_2+\omega) \tag{30}$$

$$\Rightarrow \frac{\Lambda\beta_1}{q_1} < q_2 + \omega \Rightarrow \frac{\Lambda\beta_1}{q_1} < q_2 + \omega + q_3 \Rightarrow q_2 + \omega + q_3 - \frac{\Lambda\beta_1}{q_1} > 0. \tag{31}$$

Therefore, by applying the Routh–Hurwitz stability criterion, all eigenvalues of the Jacobian matrix $J(E_0)$ have negative real parts if and only if $R_{01} < 1$ and $R_{02} < 1$. This implies that E_0 is locally asymptotically stable when

$$R_0 = \max\{R_{01}, R_{02}\} < 1. \tag{32}$$

Conversely, if $R_0 > 1$, then E_0 becomes unstable.

□

Theorem 4 The first-strain–free HBV equilibrium point E_1 of system (1) is LAS if $R_{02} > R_{01}$.

Proof. At E_1 the Jacobian matrix of the HBV system (1) is:

$$J(E_1) = \begin{bmatrix} -q_1 - \beta_2(A_2^* + C_2^*\rho_2) & -\beta_1 S^* & -S^*\beta_1\rho_1 & -S^*\beta_2 & -S^*\beta_2\rho_2 & 0 \\ 0 & -q_2 + S^*\beta_1 - \omega & S^*\beta_1\rho_1 & 0 & 0 & 0 \\ 0 & \theta_1 & -q_3 & 0 & 0 & 0 \\ \beta_2(A_2^* + C_2^*\rho_2) & \omega & 0 & S^*\beta_2 - q_4 & S^*\beta_2\rho_2 & 0 \\ 0 & 0 & 0 & \theta_2 & -q_5 & 0 \\ \nu & \gamma_1 & \gamma_2 & \gamma_3 & \gamma_4 & -\mu_1 \end{bmatrix}. \tag{33}$$

The characteristic equation of $J(E_1)$ is given by:

$$(\lambda^2 + a_1\lambda + a_2)\left[\lambda^3 + a_3\lambda^2 + a_4\lambda + a_5\right](\lambda + \mu_1) = 0, \tag{34}$$

where

$$a_1 = q_2 + q_3 + \omega - \frac{q_4 q_5 \beta_1}{q_5\beta_2 + \beta_2\theta_2\rho_2},\ a_2 = \frac{q_1 q_3 q_4 q_5 (q_2 + \omega)}{\Lambda\beta_2(q_5 + \theta_2\rho_2)}[R_{02} - R_{01}], \tag{35}$$

$$a_3 = \frac{q_4\theta_2\rho_1}{q_5 + \theta_1\rho_2} + \beta_2(A_2^* + C_2^*\rho_2) + q_1 + q_5,\ a_4 = q_1\left(\frac{q_4\theta_2\rho_2}{q_5 + \theta_1\rho_2} + q_5\right) + \beta_2(A_2^* + C_2^*\rho_2)(q_4 + q_5), \tag{36}$$

$$a_5 = \beta_2 q_4 q_5 (A_2^* + C_2^*\rho_2). \tag{37}$$

From the characteristic equations, we obtain $\lambda_1 = -\mu_1$. One can observe that the roots of $\lambda^2 + a_1\lambda + a_2 = 0$ are real and negative if $a_1 > 0$ and $a_2 > 0$, a condition that holds when $R_{02} > R_{01}$. Similarly, for the cubic equation $\lambda^3 + a_3\lambda^2 + a_4\lambda + a_5 = 0$ the Routh-Hurwitz stability conditions require that all coefficients a_3, a_4, and a_5 are positive, and that the inequality $a_3 a_4 > a_5$ is satisfied. Under these conditions, all roots of the cubic equation have negative real parts, indicating local asymptotic stability. Therefore, the first-strain–free HBV equilibrium point of system (1) is (LAS) if $R_{02} > R_{01}$. Biologically, when $R_{02} > R_{01}$, it indicates that the second HBV strain has a higher transmission potential than the first. A larger R_{02} implies a higher likelihood that the second HBV strain can persist and spread within the population. As a consequence, the first strain becomes less competitive and is unable to maintain its presence. The system naturally evolves toward a state in which only the second strain persists while the first dies out. This behavior leads to the local asymptotic stability of the strain-1-free equilibrium. From an epidemiological perspective, the strain with the larger reproduction number tends to dominate the dynamics, while the strain with the smaller R_0 cannot invade or persist when rare. □

Theorem 5 The endemic HBV equilibrium point E_2 of system (1) is LAS if $R_0 > 1$.

Proof. At E_2 the Jacobian matrix of the HBV system (1) is:

$$J(E_2)=\begin{bmatrix} -q_1-\beta_1(A_1^{**}+C_1^{**}\rho_1)-\beta_2(A_2^{**}+C_2^{**}\rho_2) & -\beta_1 S^{**} & -S^{**}\beta_1\rho_1 & -S^{**}\beta_2 & -S^{**}\beta_2\rho_2 & 0 \\ \beta_1(A_1^{**}+C_1^{**}\rho_1) & -q_2+S^{**}\beta_1-\omega & S^{**}\beta_1\rho_1 & 0 & 0 & 0 \\ 0 & \theta_1 & -q_3 & 0 & 0 & 0 \\ \beta_2(A_2^{**}+C_2^{**}\rho_2) & \omega & 0 & S^{**}\beta_2-q_4 & S^{**}\beta_2\rho_2 & 0 \\ 0 & 0 & 0 & \theta_2 & -q_5 & 0 \\ \nu & \gamma_1 & \gamma_2 & \gamma_3 & \gamma_4 & -\mu_1 \end{bmatrix}. \quad (38)$$

The characteristic polynomial corresponding to $J(E_2)$ is expressed as:

$$(\lambda+\mu_1)[\lambda^5+b_1\lambda^4+b_2\lambda^3+b_3\lambda^2+b_4\lambda+b_5]=0, \quad (39)$$

where

$$b_1=\beta_1(A_1^{**}+C_1^{**}\rho_1-S^{**})+\beta_2(A_2^{**}+C_2^{**}\rho_2-S^{**})+q_1+q_2+q_3+q_4+q_5+\omega, \quad (40)$$

$$\begin{aligned} b_2=&\omega q_4+q_2q_4+\omega q_5+q_2q_5+q_4q_5+\omega A_1{}^{**}\beta_1+A_1{}^{**}q_2\beta_1-S^{**}q_4\beta_1+A_1{}^{**}q_4\beta_1-S^{**}q_5\beta_1+A_1{}^{**}q_5\beta_1\\ &-S^{**}\omega\beta_2+\omega A_2{}^{**}\beta_2-S^{**}q_2\beta_2+A_2{}^{**}q_2\beta_2-S^{**}q_4\beta_2+A_2{}^{**}q_4\beta_2-S^{**}q_5\beta_2+A_2{}^{**}q_5\beta_2+(S^{**})^2\beta_1\beta_2\\ &-S^{**}A_1{}^{**}\beta_1\beta_2-S^{**}A_2{}^{**}\beta_1\beta_2+q_1(\omega+q_2+q_3+q_4+q_5-S^{**}(\beta_1+\beta_2))+\omega C_1{}^{**}\beta_1\rho_1+C_1{}^{**}q_2\beta_1\rho_1\\ &+C_1{}^{**}q_4\beta_1\rho_1+C_1{}^{**}q_5\beta_1\rho_1-(S^{**})^2C_1{}^{**}\beta_1\beta_2\rho_1\\ &-S^{**}\beta_1\theta_1\rho_1+\beta_2(C_2{}^{**}(\omega+q_2+q_4+q_5-S^{**}\beta_1)-S^{**}\theta_2)\rho_2\\ &+q_3(\omega+q_2+q_4+q_5+\beta_1(A_1{}^{**}+C_1{}^{**}\rho_1-S^{**})+\beta_2(A_2{}^{**}+C_2{}^{**}\rho_2-S^{**})), \end{aligned} \quad (41)$$

$$\begin{aligned} b_3=&\omega q_4q_5+q_2q_4q_5+\omega A_1{}^{**}q_4\beta_1+A_1{}^{**}q_2q_4\beta_1+\omega A_1{}^{**}q_5\beta_1+A_1{}^{**}q_2q_5\beta_1-S^{**}q_4q_5\beta_1\\ &+A_1{}^{**}q_4q_5\beta_1+\omega A_2{}^{**}q_4\beta_2+A_2{}^{**}q_2q_4\beta_2-S^{**}\omega q_5\beta_2+\omega A_2{}^{**}q_5\beta_2-S^{**}q_2q_5\beta_2+A_2{}^{**}q_2q_5\beta_2\\ &-S^{**}A_1{}^{**}q_2\beta_1\beta_2-S^{**}A_2{}^{**}q_4\beta_1\beta_2+(S^{**})^2q_5\beta_1\beta_2-S^{**}A_1{}^{**}q_5\beta_1\beta_2-S^{**}A_2{}^{**}q_5\beta_1\beta_2\\ &+\omega C_1{}^{**}q_4\beta_1\rho_1+C_1{}^{**}q_2q_4\beta_1\rho_1+\omega C_1{}^{**}q_5\beta_1\rho_1+C_1{}^{**}q_2q_5\beta_1\rho_1+C_1{}^{**}q_4q_5\beta_1\rho_1 \end{aligned}$$

$$
\begin{aligned}
&- S^{**}{C_1}^{**}q_5\beta_1\beta_2\rho_1 - S^{**}{C_1}^{**}q_2\beta_1\beta_2\rho_1 - S^{**}q_4\beta_1\theta_1\rho_1 - S^{**}q_5\beta_1\theta_1\rho_1 + (S^{**})^2\beta_1\beta_2\theta_1\rho_1 \\
&- S^{**}{A_2}^{**}\beta_1\beta_2\theta_1\rho_1 + \beta_2\Big({C_2}^{**}\big(q_5(\omega+q_2-S^{**}\beta_1)+q_4(\omega+q_2+q_5-s^{**}\beta_1)\big) - S^{**}\beta_1\theta_1\rho_1\Big) \\
&+ S^{**}\theta_2\left(-\omega-q_2+\beta_1(S^{**}-{A_1}^{**}-{C_1}^{**}\rho_1)\right)\rho_2 + \\
&+ q_1\left(\omega q_5+q_2q_5-s^{**}q_5\beta_1+q_4(\omega+q_2+q_5-S^{**}\beta_1)-S^{**}\omega\beta_2-S^{**}q_2\beta_2\right. \\
&\left.+S^{**}q_5\beta_2+(S^{**})^2\beta_1\beta_2+q_3(\omega+q_2+q_4+q_5-S^{**}(\beta_1+\beta_2))-S^{**}\beta_1\theta_1\rho_1-S^{**}\beta_2\theta_2\rho_2\right) \\
&+ q_3\left(\omega{A_1}^{**}\beta_1+{A_1}^{**}q_2\beta_1-S^{**}\omega\beta_2+\omega{A_2}^{**}\beta_2-S^{**}q_2\beta_2+{A_2}^{**}q_2\beta_2+(S^{**})^2\beta_1\beta_2\right. \\
&-S^{**}{A_1}^{**}\beta_1\beta_2-S^{**}{A_2}^{**}\beta_1\beta_2+\omega{C_1}^{**}\beta_1\rho_1+{C_1}^{**}q_2\beta_1\rho_1-S^{**}{C_1}^{**}\beta_1\beta_2\rho_1 \\
&\left.+\beta_2\left({C_2}^{**}(\omega+q_2-S^{**}\beta_1)-s^{**}\theta_2\right)\rho_2\right) \\
&+ q_4\left(\omega+q_2+q_5+\beta_1({A_1}^{**}+{C_1}^{**}\rho_1-S^{**})+\beta_2({A_2}^{**}+{C_2}^{**}\rho_2)\right) \\
&+ q_5\left(\omega+q_2+\beta_1({A_1}^{**}+{C_1}^{**}\rho_1-S^{**})+\beta_2({A_2}^{**}+{C_2}^{**}\rho_2-D^{**})\right), \qquad (42)
\end{aligned}
$$

$$
\begin{aligned}
b_4 =&\omega{A_1}^{**}q_4q_5\beta_1+{A_1}^{**}q_2q_4q_5\beta_1+\omega{A_2}^{**}q_4q_5\beta_2+{A_2}^{**}q_2q_4q_5\beta_2-S^{**}{A_1}^{**}q_2q_5\beta_1\beta_2 \\
&- S^{**}{A_2}^{**}q_4q_5\beta_1\beta_2+\omega{C_1}^{**}q_4q_5\beta_1\rho_1+{C_1}^{**}q_2q_4q_5\beta_1\rho_1-S^{**}{C_1}^{**}q_2q_5\beta_1\rho_1-S^{**}q_4q_5\beta_1\theta_1\rho_1 \\
&- S{A_2}^{**}q_4\beta_1\beta_2\theta_1\rho_1+(S^{**})^2q_5\beta_1\beta_2\theta_1\rho_1-S^{**}{A_2}^{**}q_5\beta_1\beta_2\theta_1\rho_1+\omega{C_2}^{**}q_4q_5\beta_2\rho_2 \\
&+ {C_2}^{**}q_2q_4q_5\beta_2\rho_2-S^{**}{C_2}^{**}q_4q_5\beta_1\beta_2\rho_2-S^{**}{A_1}^{**}q_2\beta_1\beta_2\theta_2\rho_2 \\
&- S^{**}{C_1}^{**}q_2\beta_1\beta_2\theta_2\rho_2+(S^{**})^2\beta_1\beta_2\theta_2\rho_2 \\
&+ q_3\left(q_4(\omega+q_2+q_5-S^{**}\beta_1)+q_5(\omega+q_2-S^{**}(\beta_1+\beta_2))-S^{**}\beta_1\theta_1\rho_1\right) \\
&+ S^{**}\left(-q_5\left((\omega+q_2-S^{**}\beta_1)\beta_2+\beta_1(S^{**}\beta_1\theta_1\rho_1)\right)-(\omega+q_2-S^{**}\beta_1)\theta_2\rho_2\right) \\
&+ q_3\left(-S^{**}\omega q_5\beta_2+\omega{A_2}^{**}q_5\beta_2-S^{**}q_2q_5\beta_2+{A_2}^{**}q_2q_5\beta_2+(S^{**})^2q_5\beta_1\beta_2-S^{**}{A_2}^{**}\beta_1\beta_2+\omega{C_1}^{**}q_5\beta_1\rho_1\right.
\end{aligned}
$$

$$+C_1{}^{**}q_2q_5\beta_1\rho_1 - S^{**}C_1{}^{**}q_2\beta_1\rho_1) + \beta_2\left((\omega+q_2-S^{**}\beta_1)(C_2{}^{**}q_5 - S^{**}\theta_2) - S^{**}C_1{}^{**}\beta_1\theta_2\rho_1\right)\rho_2$$

$$+A_1{}^{**}\beta_1\left(q_5(\omega+q_2-S^{**}\beta_2) - S^{**}\beta_2(q_2+\theta_2\rho_2)\right) + q_4\left(A_1{}^{**}(\omega+q_2)\beta_1 + \omega A_2{}^{**}q_2\beta_2\right.$$

$$\left.+A_2{}^{**}q_2\beta_2 - S^{**}A_2{}^{**}\beta_1\beta_2 + \omega C_1{}^{**}\beta_1\rho_1 + C_1{}^{**}q_2\beta_1\rho_1 + C_2{}^{**}(\omega+q_2-S^{**}\beta_1)\beta_2\rho_2\right)$$

$$+q_5\left(\omega+q_2+\beta_1(A_1{}^{**}+C_1{}^{**}\rho_1-S^{**}) + \beta_2(A_2{}^{**}+C_2{}^{**}\rho_2-S^{**})\right), \tag{43}$$

$$b_5 = q_5\left(A_1{}^{**}q_3\beta_1\left((\omega+q_2)q_4 - S^{**}q_2\beta_2\right) + C_1{}^{**}q_3\beta_1\left((\omega+q_2)q_4 - S^{**}q_2\beta_2\right)\rho_1\right.$$

$$+A_2{}^{**}q_4\beta_2\left(q_3(\omega+q_2-S^{**}\beta_1) - S^{**}\beta_1\theta_1\rho_1\right))$$

$$\left.+\beta_2\left(-S^{**}q_2q_3\beta_1\theta_2(A_1{}^{**}+C_1{}^{**}\rho_1) + C_2{}^{**}q_4q_5\left(q_3(\omega+q_2-S^{**}\beta_1) - S^{**}\beta_1\theta_1\rho_1\right)\right)\rho_2\right.$$

$$-q_1\left(q_3(\omega+q_2-S^{**}\beta_1) - S^{**}\beta_1\theta_1\rho_1\right)\left(-q_4q_5 + S^{**}\beta_2(q_5+\theta_2\rho_2)\right). \tag{44}$$

According to the Hurwitz criterion, all roots of the characteristic Eq (39) have negative real parts, and consequently, the endemic equilibrium point E_2 is (LAS) if:

$$b_1 > 0, \quad b_1b_2 - b_3 > 0, \quad b_5 > 0, \quad b_3(b_1b_2 - b_3) - b_1(b_1b_4 - b_5) > 0, \tag{45}$$

$$(b_1b_2 - b_3)(b_3b_4 - b_2b_5) + (b_1b_4 - b_5)(b_5 - b_1b_4) > 0, \tag{46}$$

and $R_0 > 1$. □

The Local Asymptotic Stability (LAS) results for the equilibrium points E_0, E_1 and E_2, as stated in Theorems 3-5, are consistent with the findings reported in multi-strain models in the literature, particularly the recent work in [48]. Theorem 3 confirms that the HBV-free equilibrium E_0 is (LAS) if $R_0 < 1$, which aligns with the condition for global asymptotic stability of the disease-free state in [48]. Theorem 5 establishes the (LAS) of the strain-2 endemic equilibrium E_2 when $R_0 > 1$, indicating persistence of the dominant strain, consistent with the findings in [48]. Theorem 5 also asserts the (LAS) of the first-strain–free equilibrium E_1 under the condition $R_{02} > R_{01}$, which is in agreement with the competitive exclusion results presented in [48].

4.3.2 *Global stability*

To study the global stability of the HBV-free equilibrium point, we employ the method adopted in [51]. Let X represent the number of uninfected individuals, defined as $X = (S, R)$. Similarly, let I denote the number of infected individuals, including acute and chronic cases of both strains, given by $I = (A_1, C_1, A_2, C_2)$. The HBV-free equilibrium is expressed as $E_0 = (X^*, 0)$, where X^* represents the equilibrium in the absence of HBV. The equilibrium E_0 is globally asymptotically stable (GAS) if the following conditions hold:

1. $\mathbf{H_1}$: The equilibrium X^* is (GAS) for the system:

$$\frac{dX}{dt} = \dot{P}(X, 0). \tag{47}$$

2. $\mathbf{H_2}$: The function $G(X, I)$ satisfies

$$G(X, I) = BI - \hat{G}(X, 0) \geq 0, \quad \forall (X, I) \in \Omega, \tag{48}$$

where:

- $B = \frac{\partial G}{\partial I}(X^*, 0)$ is a Metzler matrix.
- Ω is the domain where the model is biologically significant.

If these conditions are satisfied for the system (1), the following theorem can be applied.

Theorem 6 The HBV-free equilibrium point E_0 of the system (1) is (GAS) if $R_0 < 1$ and conditions (H_1) and (H_2) are satisfied.

Proof.

For condition (H_1), let $X = (S, R)$. We have the following:

$$P(X, I) = \begin{pmatrix} \Lambda - \beta_1 S A_1 - \beta_1 S \rho_1 C_1 - \beta_2 S A_2 - \beta_2 S \rho_2 C_2 - q_1 \\ \gamma_1 A_1 + \gamma_2 C_1 + \gamma_3 A_2 + \gamma_4 C_2 + \gamma S - \mu_1 R \end{pmatrix}. \tag{49}$$

At equilibrium $E_0 = (X^*, 0)$, we obtain:

$$P(X, 0) = \begin{pmatrix} \Lambda - q_1 S \\ \gamma S - \mu_1 R \end{pmatrix}. \tag{50}$$

By taking the partial derivatives, we get the following:

$$\dot{P}(X, 0) = \begin{pmatrix} -q_1 & 0 \\ \gamma & -\mu_1 \end{pmatrix}. \tag{51}$$

The eigenvalues of this matrix are as follows.

$$\lambda_1 = -q_1, \quad \lambda_2 = -\mu_1. \tag{52}$$

Thus, condition H_1 is satisfied. Additionally, for condition H_2, where:

$$G(X, I) = (A_1, C_1, A_2, C_2), \tag{53}$$

We have:

$$G(X,0)=\begin{bmatrix}\beta_1(A_1+\rho_1C_1)S-(\gamma_1+q_2)A_1-\omega A_1 & \theta_1A_1-(\gamma_2+q_3)C_1\\ \beta_2S(A_2+\rho_2C_2)-q_4A_2+\omega A_1 & \theta_2A_2-q_5C_2\end{bmatrix}. \tag{54}$$

From this, we obtain:

$$\frac{\partial G}{\partial I}(X^*,0)=\begin{bmatrix}\beta_1S_0^*-q_2-\omega & \beta_1S_0^*\rho_1 & 0 & 0\\ \theta_1 & -q_3 & 0 & 0\\ \omega & 0 & \beta_2S_0^*-q_4 & \beta_2S_0^*\rho_2\\ 0 & 0 & \theta_2 & -q_5\end{bmatrix}. \tag{55}$$

Since the off-diagonal elements of the matrix $B=\frac{\partial G}{\partial I}(X^*,0)$ are nonnegative, the matrix B satisfies the conditions of a Metzler matrix. Consequently, from the equation: $\hat{G}(X,I)=BI-G(X,I),$ we obtain:

$$\hat{G}(X,I)=\begin{bmatrix}\beta_1A_1(S_0^*-S)+\beta_1\rho_1C_1(S_0^*-S)\\ 0\\ \beta_2A_2(S_0^*-S)+\beta_2\rho_2C_2(S_0^*-S)\\ 0\end{bmatrix}. \tag{56}$$

It is well established that if $S_0^*>S$, then $\hat{G}(X,I)\geq 0$ for all $(X,I)\in\Omega$, thereby ensuring the validity of condition (H2). Consequently, disease-free equilibrium is proven to be (GAS) whenever $R_0<1$, provided that both conditions (H1) and (H2) are satisfied, as has been verified formally. □

In the following Section, global stability will be established using an alternative approach, namely the Lyapunov function method, as demonstrated in the next theorem.

Theorem 7 The disease-free equilibrium point E_0 of the HBV system (1) is (GAS) if $R_0<1$.

Proof. Consider the following Lyapunov function V defined as follows:

$$V=A_1+\frac{\beta_1\rho_2\Lambda}{q_1q_3}C_1+A_2+\frac{\beta_2\rho_2\Lambda}{q_1q_5}C_2. \tag{57}$$

To compute the time derivative of the Lyapunov function, we differentiate it along the system's trajectories as follows:

$$\begin{aligned}\dot{V} =&\beta_1 S(A_1+\rho_1 C_1)-(q_2+\omega)A_1+\frac{\beta_1\rho_1\Lambda}{q_1q_3}[\theta_1A_1-q_3C_1]\\ &+\beta_2 S(A_2+\rho_2C_2)-q_4A_2+\omega A_1+\frac{\beta_2\rho_2\Lambda}{q_1q_5}[\theta_2A_2-q_5C_2]\\ \leq&\beta_1 S_0^*(A_1+\rho_1 C_1)-(q_2+\omega)A_1+\frac{\beta_1\rho_1\Lambda}{q_1q_3}[\theta_1A_1-q_3C_1]\\ &+\beta_2 S_0^*(A_2+\rho_2C_2)-q_4A_2+\omega A_1+\frac{\beta_2\rho_2\Lambda}{q_1q_5}[\theta_2A_2-q_5C_2]\\ \leq&[\frac{\beta_1\Lambda}{q_1}+\frac{\beta_1\rho_1\Lambda\theta_1}{q_1q_3}-q_2]A_1+[\frac{\beta_2\Lambda}{q_1}+\frac{\beta_2\rho_2\Lambda\theta_2}{q_1q_5}-q_5]A_2\leq q_2[R_{01}-1]A_1+q_4[R_{02}-1]A_2.\end{aligned} \tag{58}$$

Thus, $\dot{V}<0$ if $R_0<1$, indicating that E_0 is (GAS). □

Theorem 8 The first-strain–free equilibrium point of system (1) is (GAS) if $R_{02}>R_{01}$.

Proof. Let the Lyapunov function V be defined as:

$$V=(S-S^*-S^*\ln\frac{S}{S^*})+D_1A_1+D_2C_1+(A_2-A_2^*-A^*\ln\frac{A_2}{A_2^*})+D_3(C_2-C_2^*-C_2^*\ln\frac{C_2}{C_2^*}), \tag{59}$$

where D_1, D_2 and D_3 are positive constant, defined as follows:

$$D_1=\frac{\beta_1S^*(q_3+\rho_1\theta_1)}{q_3(q_2+\omega)},\ D_2=\frac{\rho_1\beta_1S^*}{q_3},\ D_3=\frac{\beta_1S^*C_2^*\rho_2}{\theta_1A_2^*}. \tag{60}$$

Thus:

$$\begin{aligned}\dot{V}=&\left(1-\frac{S^*}{S}\right)(\Lambda-\beta_2S(A_2+\rho_2C_2)-q_1S-\beta_1S(A_1+\rho_1C_1))\\ &+D_1\beta_1S(A_1+\rho_1C_1)-D_1A_1(q_2+\omega)+D_2(\theta_1A_1+q_3C_1)\\ &+\left(1-\frac{A_2^*}{A_2}\right)(\beta_2S(A_2+\rho_2C_2)-q_4A_2)+D_3\left(1-\frac{C_2^*}{C_2}\right)(\theta_2A_2-q_5C_2).\end{aligned} \tag{61}$$

At the equilibrium point E_1, the system yields:

$$\Lambda = \beta_2 S^*(A_2^* + \rho_2 C_2^*) + q_1 S^*,$$

$$q_4 = \frac{\beta_2 S^*(A_2^* + \rho_2 C_2^*)}{A_2^*}, \tag{62}$$

$$q_5 = \frac{\theta_2 A_2^*}{C_2^*}.$$

By substituting (62) into (61) and using the previously defined values of D_1, D_2 and D_3, we obtain the following expression:

$$\begin{aligned}\dot{V} =& -\frac{q_1}{S}(S-S^*)^2 - \beta_2 S^* A_2^* \left(\frac{S^*}{S} + \frac{S}{S^*} - 2\right) \\ & - \beta_2 S^* C_2^* \rho_2 \left(\frac{S^*}{S} + \frac{C_2^* A_2}{C_2 A_2^*} + \frac{A_2^* S C_2}{A_2 S^* C_2^*} - 3\right) \\ & - \beta_1 S(A_1 + \rho_1 C_1) + \left(\frac{\beta_1 S^*(q_3 + \rho_1 \theta_1)}{q_3(q_2+\omega)}\right) \beta_1 S(A_1 + \rho_1 C_1).\end{aligned} \tag{63}$$

Given that $S^* = \frac{\Lambda}{q_1 R_{02}}$ at E_1, we obtain the following:

$$\begin{aligned}\dot{V} =& -\frac{q_1}{S}(S-S^*)^2 - \beta_2 S^* A_2^* \left(\frac{S^*}{S} + \frac{S}{S^*} - 2\right) - \beta_2 S^* C_2^* \rho_2 \left(\frac{S^*}{S} + \frac{C_2^* A_2}{C_2 A_2^*} + \frac{A_2^* S C_2}{A_2 S^* C_2^*} - 3\right) \\ & - \beta_1 S(A_1 + \rho_1 C_1)(1 - \frac{R_{01}}{R_{02}}).\end{aligned} \tag{64}$$

Under the condition that $R_{02} > R_{01}$, $\dot{V} \leq 0$, thereby satisfying the requirement for global stability. Consequently, the free first strain equilibrium E_1 is (GAS). □

Theorem 9 The endemic equilibrium point E_2 of system (1) is (GAS) if $R_0 > 1$.

Proof. Let the Lyapunov function V be defined as:

$$\begin{aligned}V =& (S - S^{**} - S^{**} \ln \frac{S}{S^{**}}) + (A_1 - A_1^{**} - A_1^{**} \ln \frac{A_1}{A_1^{**}}) + D_4(C_1 - C_1^{**} - C_1^{**} \ln \frac{C_1}{C_1^{**}}) \\ & (A_1 - A_2^{**} - A_1^{**} \ln \frac{A_2}{A_2^{**}}) + D_5(C_2 - C_2^{**} - C_2^{**} \ln \frac{C_2}{C_2^{**}}),\end{aligned} \tag{65}$$

where

$$D_4 = \frac{\rho_1\beta_1 S^{**}C_1^{**}}{\theta_1 A_1^{**}},\ D_5 = \frac{\rho_2\beta_2 S^{**}C_2^{**}}{\theta_2 A_2^{**}}, \tag{66}$$

Thus:

$$\dot{V} = (1-\frac{S^{**}}{S})\dot{S} + (1-\frac{A_1^{**}}{A_1})\dot{A_1} + D_4(1-\frac{C_1^{**}}{C_1})\dot{C_1} + (1-\frac{A_2^{**}}{A_2})\dot{A_2} + D_5(1-\frac{C_2^{**}}{C_2})\dot{C_2}. \tag{67}$$

At the equilibrium point E_2, we have:

$$\begin{aligned}
\dot{V} =& -\frac{q_1}{S}(S^{**}-S)^2 + \beta_1 S^{**}A_1^{**}[1-\frac{S^{**}}{S}-\frac{SA_1}{S^{**}A_1^{**}}+\frac{A_1}{A_1^{**}}] + \beta_1 S^{**}\rho_1 C_1^{**}[1-\frac{S^{**}}{S}-\frac{SC_1}{S^{**}C_1^{**}}+\frac{C_1}{C_1^{**}}] \\
&+ \beta_2 S^{**}A_2^{**}[1-\frac{S^{**}}{S}-\frac{SA_2}{S^{**}A_2^{**}}+\frac{A_2}{A_2^{**}}] + \beta_2 S^{**}\rho_2 C_2^{**}[1-\frac{S^{**}}{S}-\frac{SC_2}{S^{**}C_2^{**}}+\frac{C_2}{C_2^{**}}] \\
&+ (1-\frac{A_1^{**}}{A_1})[\beta_1 S^{**}A_1^{**}(\frac{SA_1}{S^{**}A_1^{**}}-\frac{A_1}{A_1^{**}}) + \beta_1 S^{**}\rho_1 C_1^{**}(\frac{SC_1}{S^{**}C_1^{**}}-\frac{A_1}{A_1^{**}})] \\
&+ D_4\theta_1 A_1[\frac{A_1}{A_1^{**}}-\frac{A_1C_1^{**}}{A_1^{**}C_1}-\frac{C_1}{C_1^{**}}+1] \\
&+ (1-\frac{A_2^{**}}{A_2})[\beta_2 S^{**}A_2^{**}(\frac{SA_2}{S^{**}A_2^{**}}-\frac{A_2}{A_2^{**}}) + \beta_2 S^{**}\rho_2 C_2^{**}(\frac{SC_2}{S^{**}C_2^{**}}-\frac{A_2}{A_2^{**}})] \\
&+ D_5(1-\frac{C_2^{**}}{C_2})[\theta_2 A_2 - q_5 C_2].
\end{aligned} \tag{68}$$

Incorporating the expressions of D_4 and D_5 into the equation leads to the following result.

$$\begin{aligned}
\dot{V} =& -\frac{q_1}{S}(S^{**}-S)^2 - \beta_1 S^{**}A_1^{**}[\frac{S^{**}}{S}+\frac{S}{S^{**}}-2] - \beta_1 S^{**}\rho_1 C_1^{**}[\frac{S^{**}}{S}-\frac{A_1C_1^{**}}{A_1^{**}C_1}-\frac{SA_1^{**}C_1}{S^{**}A_1C_1^{**}}] \\
&- \beta_2 S^{**}A_2^{**}[\frac{S^{**}}{S}+\frac{S}{S^{**}}-2] - \beta_2 S^{**}\rho_2 C_2^{**}[\frac{S^{**}}{S}+\frac{A_2C_2^{**}}{A_2^{**}C_2}+\frac{SA_2^{**}C_2}{S^{**}A_2C_2^{**}}-3].
\end{aligned} \tag{69}$$

By applying the inequality of arithmetic and geometric means, we obtain $\dot{V} \leq 0$, which implies that E_2 of the HBV model is (GAS). □

5. Bifurcation analysis

In the following Section, forward and backward bifurcation of the hepatitis B infection model will be investigated. To achieve this, we employ the Center Manifold Theory (CMT) [52]. Firstly, the state variables are redefined as $x_1 = S$, $x_2 = A_1$, $x_3 = C_1$, $x_4 = A_2$, $x_5 = C_2$, and $x_6 = R$. Utilizing vector notation, they can be expressed as $\mathbf{x} = (x_1, x_2, x_3, x_4, x_5, x_6)^T$. Accordingly, the HBV system (1) can be formulated as follows:

$$\begin{aligned}
\frac{dx_1}{dt} &= h_1 = \Lambda - \beta_1 x_1(x_2 + \rho_1 x_3) - \beta_2 x_1(x_4 + \rho_2 x_5) - q_1 x_1,\\
\frac{dx_2}{dt} &= h_2 = \beta_1 x_1(x_2 + \rho_1 x_3) - q_2 x_2 - \omega x_2,\\
\frac{dx_3}{dt} &= h_3 = \theta_1 x_2 - q_3 x_3,\\
\frac{dx_4}{dt} &= h_4 = \beta_2 x_1(x_4 + \rho_2 x_5) - q_4 x_4 + \omega x_2,\\
\frac{dx_5}{dt} &= h_5 = \theta_2 x_4 - q_5 x_5,\\
\frac{dx_6}{dt} &= h_6 = \gamma_1 x_2 + \gamma_2 x_3 + \gamma_3 x_4 + \gamma_4 x_5 + \nu x_1 - \mu_1 x_6.
\end{aligned} \tag{70}$$

Following [52], system (70) can be written as:

$$\frac{d\mathbf{x}}{dt} = h(\mathbf{x}, \beta_2). \tag{71}$$

The Jacobian matrix of (70) evaluated in the HBV-free equilibrium is as follows:

$$J^* = \begin{bmatrix}
-q_1 & -\frac{\Lambda\beta_1}{q_1} & -\frac{\Lambda\beta_1\rho_1}{q_1} & -\frac{\Lambda\beta_2}{q_1} & -\frac{\Lambda\beta_2\rho_2}{q_1} & 0\\
0 & -\omega - q_2 + \frac{\Lambda\beta_1}{q_1} & \frac{\Lambda\beta_1\rho_1}{q_1} & 0 & 0 & 0\\
0 & \theta_1 & -q_3 & 0 & 0 & 0\\
0 & \omega & 0 & -q_4 + \frac{\Lambda\beta_2}{q_1} & \frac{\Lambda\beta_2\rho_2}{q_1} & 0\\
0 & 0 & 0 & \theta_2 & -q_5 & 0\\
\nu & \gamma_1 & \gamma_2 & \gamma_3 & \gamma_4 & -\mu_1
\end{bmatrix}. \tag{72}$$

The Jacobian matrix J^* exhibits eigenvalues with negative real parts, with the exception of a single eigenvalue that becomes zero when $R_{02} = 1$. Consequently, for the case where $R_{02} = 1$, one can utilize the CMT to investigate the bifurcation analysis of the HBV system (70) when $R_{02} = 1$, which is equivalent to $\beta_2 = \beta_2^* = \frac{q_1 q_4 q_5}{\Lambda(q_5+\theta_2\rho_2)}$. This results in the right eigenvector, which is represented as: $\mathbf{M_1} = (w_1, w_2, w_3, w_4, w_5, w_6)^T$, where

$$w_1 = -\frac{\Lambda\beta_2(q_5+\theta_2\rho_2)}{q_1^2\theta_2},\ w_2 = 0,\ w_3 = 0,\ w_4 = \frac{q_5}{\theta_2},\ w_5 = 1,\ w_6 = \frac{q_5(-\Lambda\nu\beta_2 q_1^2\gamma_3)+\theta_2(q_1^2\gamma_4-\Lambda\nu\beta_2\rho_2)}{q_1^2\theta_2\mu_1}. \tag{73}$$

Moreover, the left eigenvector of the Jacobian matrix J^* is expressed as: $\mathbf{M_2} = (v_1, v_2, v_3, v_4, v_5, v_6)$, where:

$$v_1 = 0,\ v_2 = \frac{\Lambda q_4\beta_1\theta_1\rho_1\rho_2+\omega q_1 q_3(q_5+\theta_2\rho_2)}{q_3 q_4(q_1(\omega+q_2)-\Lambda\beta_1)\rho_2},\ v_3 = \frac{\Lambda\beta_1\rho_1}{q_1 q_3},\ v_4 = \frac{q_1\theta_2}{q_1 q_4-\Lambda\beta_2},\ v_5 = 0,\ v_6 = 0. \tag{74}$$

According to [52], the local behavior of the system near the equilibrium point is characterized by the coefficients B_1 and B_2, defined as follows:

$$B_1 = \sum_{k,i,j=1}^{n} v_k w_i w_j \frac{\partial^2 h_k}{\partial x_i \partial x_j}(0,0), \tag{75}$$

$$B_2 = \sum_{k,i=1}^{n} v_k w_i \frac{\partial^2 h_k}{\partial x_i \partial \beta_2}(0,0), \tag{76}$$

where $h_k(x, \beta_2)$ the k-th component of the function h. Particularly, if $B_2 > 0$ and $B_1 > 0$, then a backward bifurcation occurs for system (1) at $\beta_2 = 0$; while $B_2 > 0$ and $B_1 < 0$, a forward bifurcation occurs.

Furthermore, by substituting the vectors M_1 and M_2 into the expression (75), (76), we obtain:

$$B_1 = -\frac{2\Lambda q_5\beta_2^2(q_5+\theta_2\rho_2)}{q_1(q_1q_4-\Lambda\beta_2)\theta_2} - \frac{2\Lambda\beta_2^2\rho_2(q_5+\theta_2\rho_2)}{q_1(q_1q_4-\Lambda\beta_2)}, \tag{77}$$

$$B_2 = \frac{\Lambda q_5}{q_1q_4-\Lambda\beta_2} + \frac{\Lambda\theta_2\rho_2}{q_1q_4-\Lambda\beta_2}. \tag{78}$$

Given that $B_1 < 0$ and $B_2 > 0$, a forward bifurcation occurs at $\beta_2 = \beta_2^*$, corresponding to the threshold $R_{02} = 1$, which is equivalent to $\beta_2 = \beta_2^* = \frac{q_1 q_4 q_5}{\Lambda(q_5+\theta_2\rho_2)}$.

6. Model analysis optimization of the biological control

Optimal control theory is a fundamental mathematical framework widely utilized in infectious disease modeling to develop effective strategies for minimizing the spread of various types of infections [53].

In this study, we apply optimal control theory to system (1) to design a control strategy aimed at reducing disease transmission. The model classifies individuals into distinct epidemiological compartments, allowing for the implementation of two primary control interventions: vaccination and treatment. The vaccination strategy u_1 targets susceptible individuals (S) to reduce the likelihood of infection, while the treatment intervention u_2 focuses on infected

individuals (A_1, C_1, A_2, C_2) to mitigate disease progression and limit its spread within the population. The objective functional $\mathscr{J}$ given by:

$$\mathscr{J} = \int_0^T [K_1A_1 + K_2C_1 + K_3A_2 + K_4C_2 + \frac{1}{2}(K_5u_1^2 + K_6u_2^2)]dt, \tag{79}$$

subject to the system:

$$\begin{aligned}
\dot{S} &= \Lambda - \beta_1 S(A_1 + \rho_1 C_1) - \beta_2 S(A_2 + \rho_2 C_2) - (u_1 + \mu_1)S, \\
\dot{A_1} &= \beta_1(A_1 + \rho_1 C_1)S - (\gamma_1 + \mu_1 + \theta_1)A_1 - \omega A_1 - u_2 A_1, \\
\dot{C_1} &= \theta_1 A_1 - (\gamma_2 + \mu_1 + \mu_2)C_1 - u_2 C_1, \\
\dot{A_2} &= \beta_2 S(A_2 + \rho_2 C_2) - (\gamma_3 + \mu_1 + \theta_2)A_2 + \omega A_1 - u_2 A_2, \\
\dot{C_2} &= \theta_2 A_2 - (\gamma_4 + \mu_1 + \mu_3)C_2 - u_2 C_2, \\
\dot{R} &= \gamma_1 A_1 + \gamma_2 C_1 + \gamma_3 A_2 + \gamma_4 C_2 + u_1 S - \mu_1 R + (A_1 + C_1 + A_2 + C_2)u_2.
\end{aligned} \tag{80}$$

The parameters K_1, K_2, K_3, and K_4 represent the relative weight constants for individuals infected with acute and chronic infections from both strains, respectively. Additionally, K_5 and K_6 denote the costs associated with vaccination and treatment. The objective functional $\mathscr{J}$ represents the total cost to be minimized, which includes the cumulative number of infected individuals (A_1, C_1, A_2, C_2) over the intervention period and the quadratic costs associated with the control efforts u_1 and u_2. The objective functional captures the trade-off between minimizing the burden of infection (via the cumulative number of infected individuals) and the economic cost of applying vaccination and treatment interventions, represented by the quadratic cost terms $u_1^2(t)$ and $u_2^2(t)$. The weights $K_1 - K_4$ quantify the relative importance of reducing different infected compartments, while K_5 and K_6 represent the unit costs of vaccination and treatment. These were selected based on standard practices in the literature and tested via sensitivity analysis to ensure the robustness of the results.

Pontryagin's Maximum Principle (PMP) provides the necessary conditions for optimality in control problems. It is a fundamental tool in optimal control theory, allowing the derivation of optimal control strategies for dynamic systems [54]. PMP is employed to derive the necessary conditions for optimality, as the system satisfies the regularity and smoothness conditions required for its application. The principle is particularly suitable for our model since the control variables u_1 and u_2 appear explicitly and influence the nonlinear dynamics of the system.

The admissible control set is defined as

$$\mathscr{U} = \{(u_1(t), u_2(t)) \in L^\infty(0, T) \times L^\infty(0, T) \,|\, 0 \le u_1(t) \le u_1^{\max},\ 0 \le u_2(t) \le u_2^{\max}\}, \tag{81}$$

where $u_1(t)$ and $u_2(t)$ are Lebesgue measurable, bounded, and piecewise continuous functions on $[0, T]$, taking values in the compact intervals $[0, u_1^{\max}]$ and $[0, u_2^{\max}]$, respectively. These standard assumptions in optimal control theory guarantee the existence of optimal solutions and allow for time-dependent, dynamically adjusted intervention strategies.

In this context, the Hamiltonian H associated with (u_1, u_2) is formulated as follows:

$$H = L + \lambda_1 \dot{S} + \lambda_2 \dot{A_1} + \lambda_3 \dot{C_1} + \lambda_4 \dot{A_2} + \lambda_5 \dot{C_2} + \lambda_6 \dot{R}, \tag{82}$$

where

$$L = K_1 A_1 + K_2 C_1 + K_3 A_2 + K_4 C_2 + \frac{1}{2}(K_5 u_1^2 + K_6 u_2^2). \tag{83}$$

The following result establishes the adjoint system, which is formulated as follows:

$$\begin{aligned} &\frac{d\lambda_1}{dt} = -\frac{\partial H}{\partial S}, \qquad \frac{d\lambda_2}{dt} = -\frac{\partial H}{\partial A_1}, \qquad \frac{d\lambda_3}{dt} = -\frac{\partial H}{\partial C_1} \\ &\frac{d\lambda_4}{dt} = -\frac{\partial H}{\partial A_2}, \qquad \frac{d\lambda_5}{dt} = -\frac{\partial H}{\partial C_2}, \qquad \frac{d\lambda_6}{dt} = -\frac{\partial H}{\partial R}. \end{aligned} \tag{84}$$

This system characterizes the evolution of the adjoint variables $\lambda_i,\ i = 1{:}\ 6$, which play a crucial role in determining the optimal control functions.

$$\begin{aligned} \lambda_1'(t) &= \beta_1\{A_1 + \rho_2 C_1\}\{\lambda_1(t) - \lambda_2(t)\} + \beta_2\{A_2 + \rho_2 C_2\}\{\lambda_1(t) - \lambda_4(t)\} \\ &\quad + u_1\{\lambda_1(t) - \lambda_6(t)\} + \mu_1 \lambda_1(t), \\ \lambda_2'(t) &= -K_1 + \lambda_2(t)\mu_1 + S\beta_1\{\lambda_1(t) - \lambda_2(t)\} + \gamma_1\{\lambda_2(t) - \lambda_6(t)\} + \theta_1\{\lambda_2(t) - \lambda_3(t)\} \\ &\quad + u_2\{\lambda_2(t) - \lambda_6(t)\} + \omega\{\lambda_2(t) - \lambda_4(t)\}, \\ \lambda_3'(t) &= -K_2 + \lambda_3(t)\{\mu_1 + \mu_2\} + \beta_1 S\rho_1\{\lambda_1(t) - \lambda_2(t)\} + u_2\{\lambda_3(t) - \lambda_6(t)\} \\ &\quad + \gamma_2\{\lambda_3(t) - \lambda_6(t)\}, \\ \lambda_4'(t) &= -K_3 + \mu_1 \lambda_4(t) + \beta_2 S\{\lambda_1(t) - \lambda_4(t)\} + \gamma_3\{\lambda_4(t) - \lambda_6(t)\} \\ &\quad + \theta_2\{\lambda_4(t) - \lambda_5(t)\} + u_2\{\lambda_4(t) - \lambda_6(t)\}, \\ \lambda_5'(t) &= -K_4 + \beta_2 S\rho_2\{\lambda_1(t) - \lambda_4(t)\} + \gamma_4\{\lambda_5(t) - \lambda_6(t)\} \\ &\quad + \lambda_5(t)\{\mu_1 + \mu_3\} + u_2\{\lambda_5(t) - \lambda_6(t)\}, \\ \lambda_6'(t) &= \mu_1 \lambda_6(t). \end{aligned} \tag{85}$$

To characterize the optimal control, we solve the following partial differential equations.

$$\frac{\partial H}{\partial u_1} = 0, \quad \frac{\partial H}{\partial u_2} = 0, \tag{86}$$

then

$$\begin{aligned} u_1^* &= \max\left\{\min\left(\frac{1}{K_5}S^*(\lambda_1-\lambda_6), 1\right), 0\right\}, \\ u_2^* &= \max\left\{\min\left(\frac{A_1^*(\lambda_2-\lambda_6)+C_1^*(\lambda_3-\lambda_6)+A_2^*(\lambda_4-\lambda_6)+C_2^*(\lambda_5-\lambda_6)}{K_6}, 1\right), 0\right\}. \end{aligned} \tag{87}$$

7. Sensitivity analysis

Sensitivity indices are an analytical tool of great importance to determine the impact of each of the model parameters. These indices are designed to identify the factors that affect the spread of the disease and influence the value of R_0, increasing or decreasing it. The sensitivity index for each coefficient is calculated as follows:

$$\Upsilon_p^{R_0} = \frac{\partial R_0}{\partial p} \times \frac{p}{R_0}, \tag{88}$$

where p represents any parameter in R_0. The indices are obtained in this manner, and the results are presented in Table 1.

Table 1. Sensitivity indices for R_0 based on parameter values

Parameter	Index value	Parameter	Index value
Λ	+1	θ_2	−0.787633
ν	−0.223964	μ_1	−0.802475
ω	−0.028496	μ_2	−0.193112
β_1	+1	μ_3	−0.169640
β_2	+1	γ_1	−0.011398
ρ_1	+0.201735	γ_2	−0.001931
ρ_2	+0.177214	γ_3	−0.012865
θ_1	−0.738624	γ_4	−0.001696

Figure 2 shows that the sensitivity indices, whose positive values indicate that the variable directly affects R_0, that is, increasing it leads to an increase in the disease transmission rate. A negative sensitivity value indicates an inverse relationship, meaning that increasing the corresponding value results in a decrease in the disease transmission rate. It also indicates that the most sensitive parameters include the vaccination rate ν, the recovery rates from both acute and chronic infections of types (1) and (2), as well as the natural and virus-induced mortality rates for both types. Additionally, the virus mutation rate is identified as a highly influential parameter.

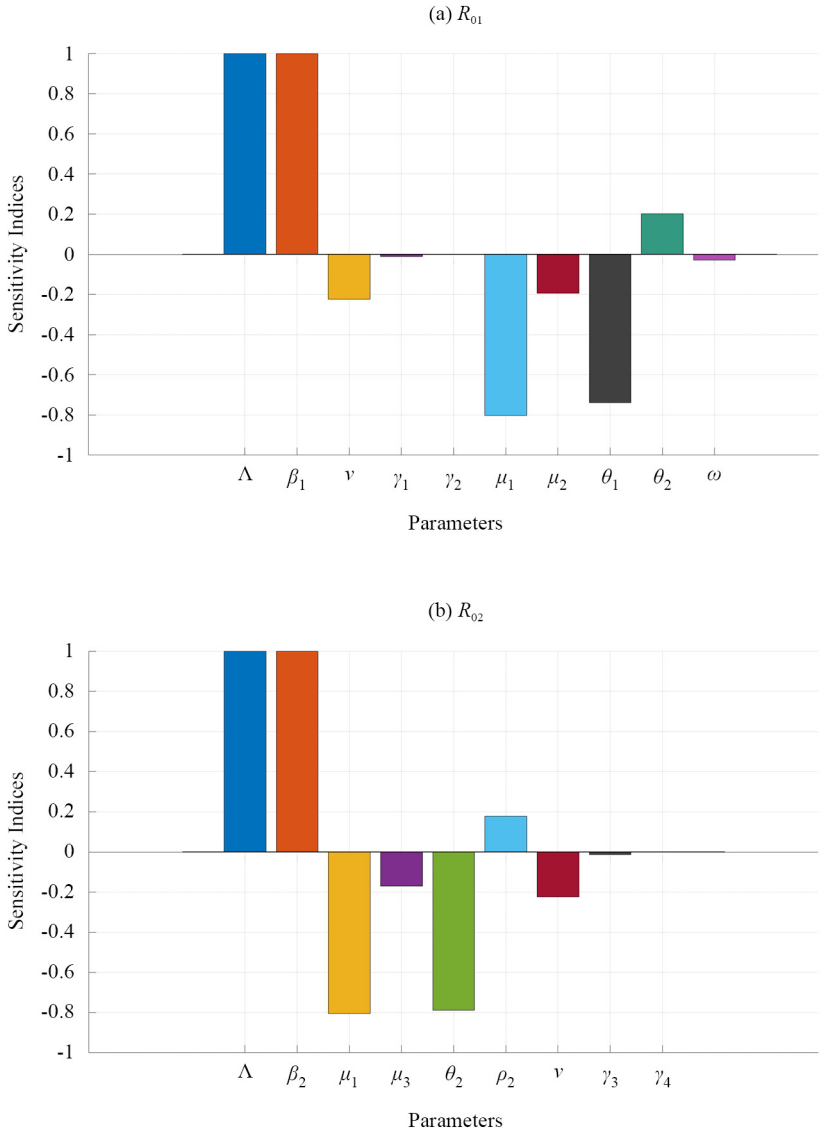

Figure 2. Sensitivity indices of R_0

8. Numerical simulations

The analytical findings are verified through numerical simulations conducted in MATLAB. The parameters employed in this work have been calibrated based on the data provided in reference [22], as follows:

$$\Lambda = 0.0121,\ \beta_1 = 0.05,\ \rho_1 = 0.16,\ \nu = 0.002,\ \mu_1 = 0.00693,\ \gamma_1 = 0.004,\ \gamma_2 = 0.002,\ \theta_1 = 0.33, \tag{89}$$

$$\mu_2 = 0.2,\ \beta_2 = 0.005,\ \rho_2 = 0.15,\ \gamma_3 = 0.004,\ \gamma_4 = 0.002,\ \theta_2 = 0.3,\ \mu_3 = 0.2,\ \omega = 0.01. \tag{90}$$

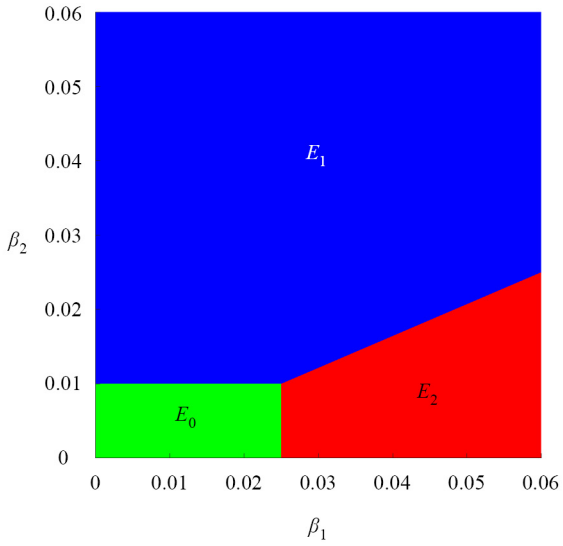

Figure 3. Stability regions in the (β_1, β_2) parameter space

Figure 3 illustrates the stability regions corresponding to three different equilibrium points of the mathematical model. The horizontal axis represents variations in the parameter β_1, while the vertical axis corresponds to variations in the parameter β_2.

The green region denotes the parameter values for which the first point E_0 is stable. The blue region indicates the stability region of the second point E_1. The red region corresponds to the stability region of the third point E_2. The boundaries separating these regions represent bifurcation thresholds, where the stability of the system changes from one equilibrium state to another due to changes in the parameter values. This classification helps identify which equilibrium configuration governs the behavior of the system under different parameter settings.

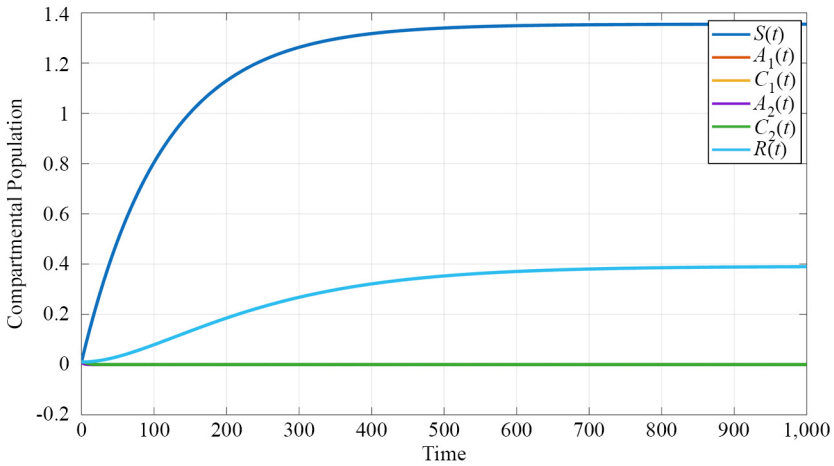

Figure 4. Simulation of the model around E_0 is presented when $R_0 < 1$

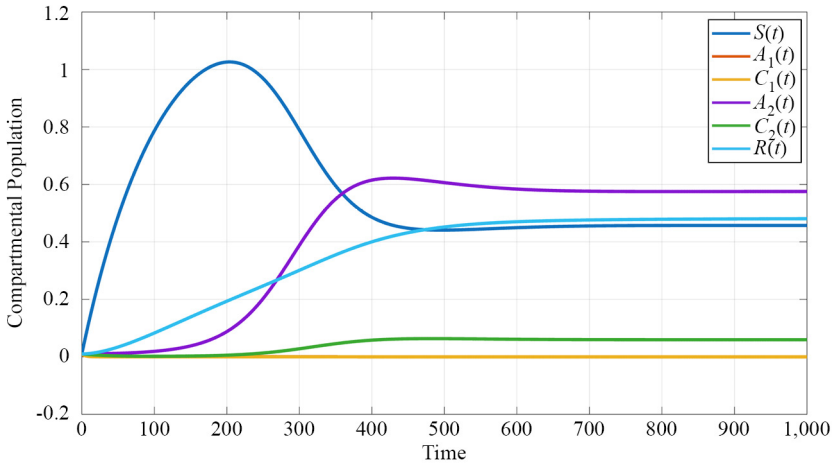

Figure 5. Simulation of the model around first-strain–free equilibrium point E_1 is presented when $R_{02} > R_{01}$

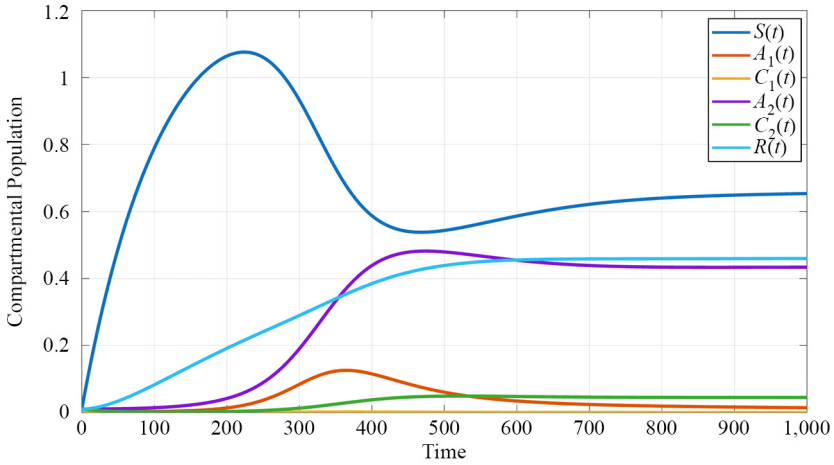

Figure 6. Simulation of the model around the endemic equilibrium E_2 is presented when $R_0 > 1$

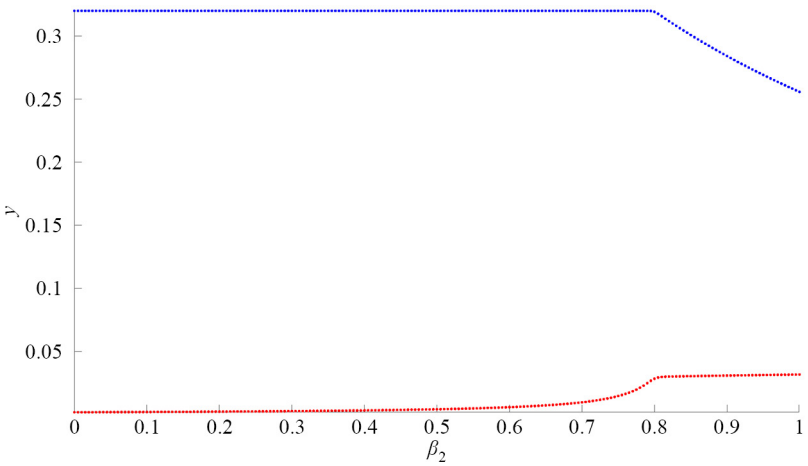

Figure 7. Forward bifurcation of the HBV model with respect to β_2

After creating the stability regions in the parameter space β_1 and β_2, we selected different values in each region that achieve the stability of our equilibrium points. In Figure 4, by selecting $\beta_1 = 0.01$ and $\beta_2 = 0.005$, we found that the solution stabilizes around the point E_0, which corresponds to Figure 3 and coincides with Theorem 8. When changing $\beta_1 = 0.03$ and $\beta_2 = 0.03$ for Figure 5, it showed that the solution stabilizes around the point E_1, which also corresponds to Figure 3 and coincides with Theorem 9. Finally, by modifying β_1 and β_2 to take the following values $\beta_1 = 0.05$ and $\beta_2 = 0.02$ for Figure 6, it achieves the stability of point E_2, which is consistent with Figure 3 and coincides with Theorem 10. The forward bifurcation in Figure 7 shows the behavior of the system as R_0 changes: When $R_0 < 1$, the first point appears as in Figure 4, while two additional points appear when $R_0 > 1$ as shown in Figures 5 and 6.

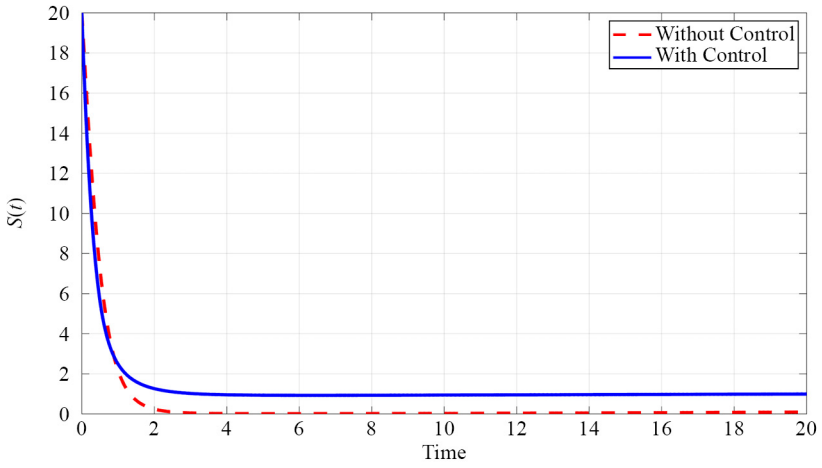

Figure 8. Dynamics of $S(t)$ with control and without control

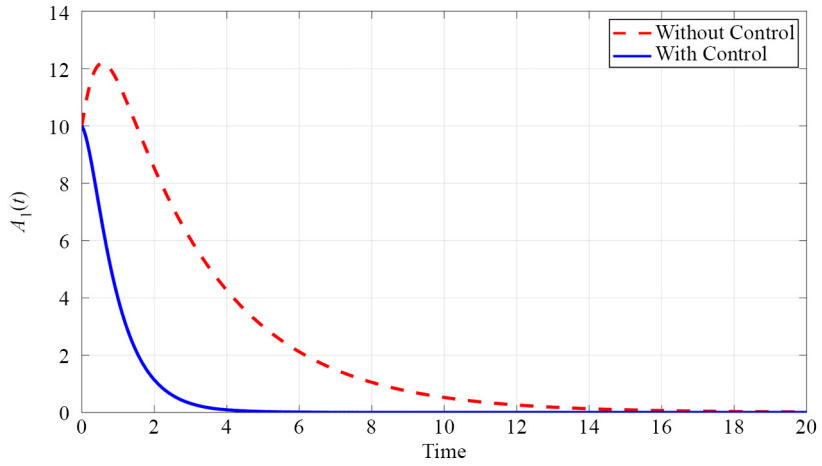

Figure 9. Dynamics of acute infection from the first strain with and without control

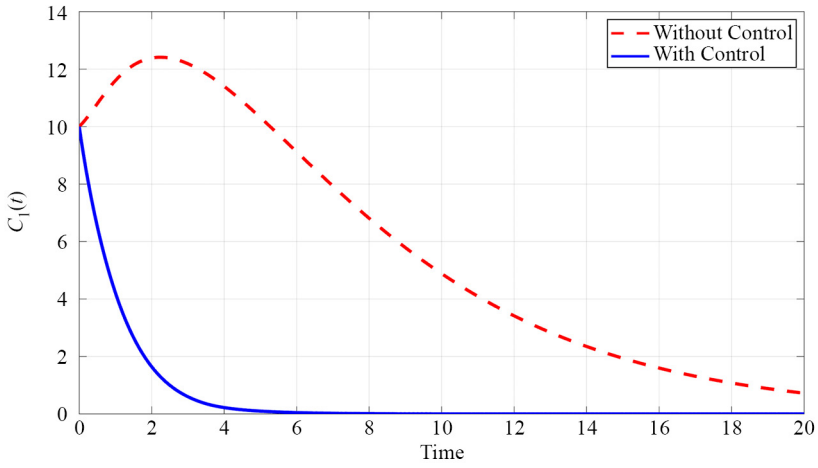

Figure 10. Dynamics of chronic infection from the first strain with and without control

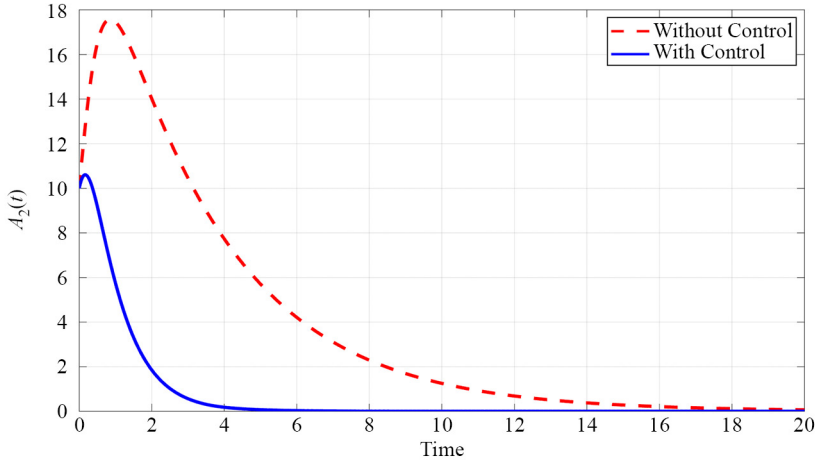

Figure 11. Dynamics of acute infection from the second strain with and without control

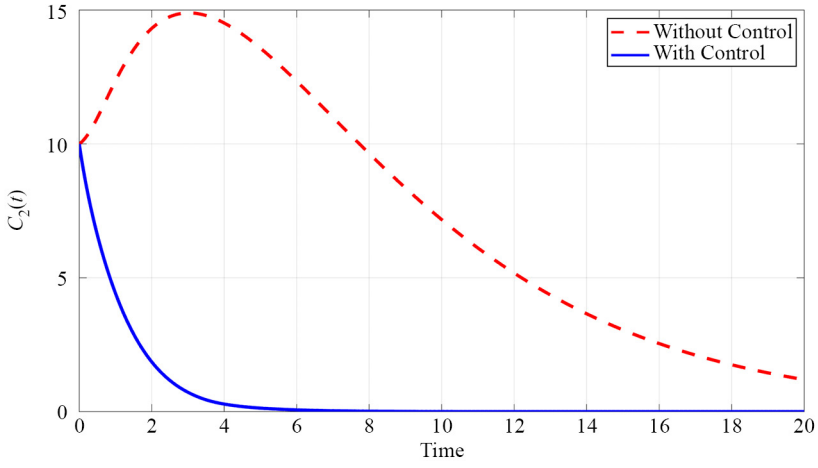

Figure 12. Dynamics of chronic infection from the second strain with and without control

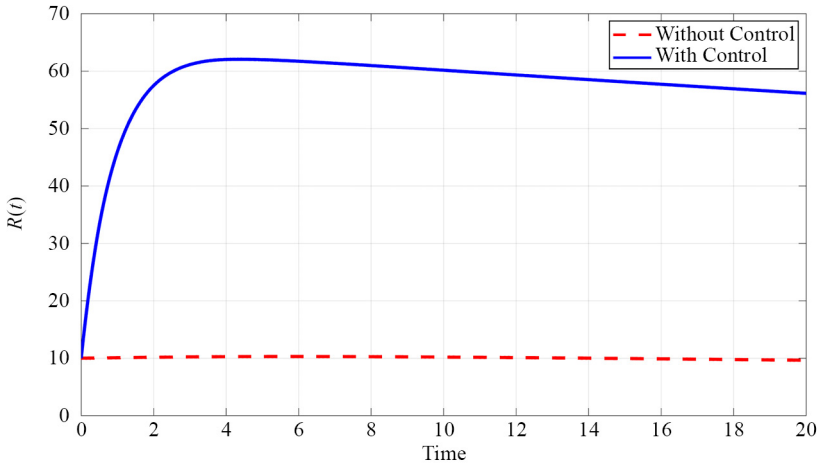

Figure 13. Dynamics of $R(t)$ with and without control

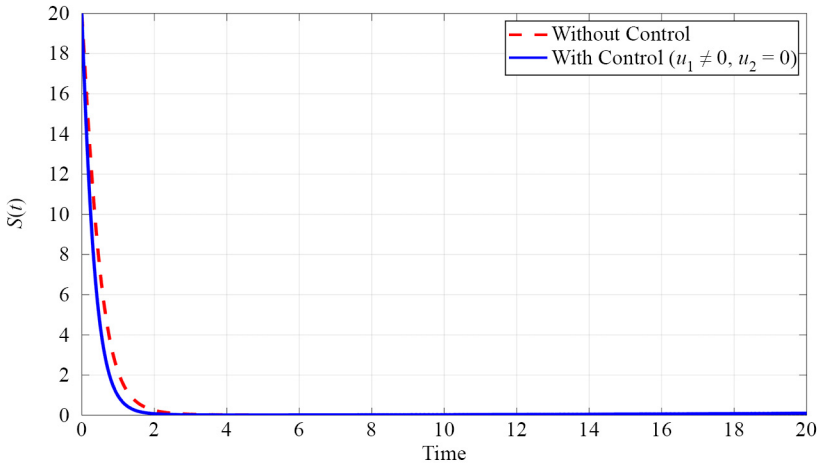

Figure 14. Dynamics of $S(t)$ when only vaccination is implemented

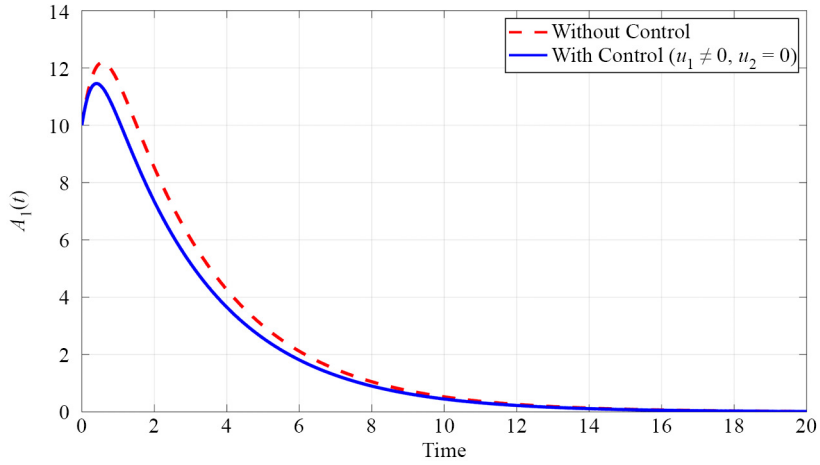

Figure 15. Dynamics of acute infection from the first strain when only vaccination is implemented

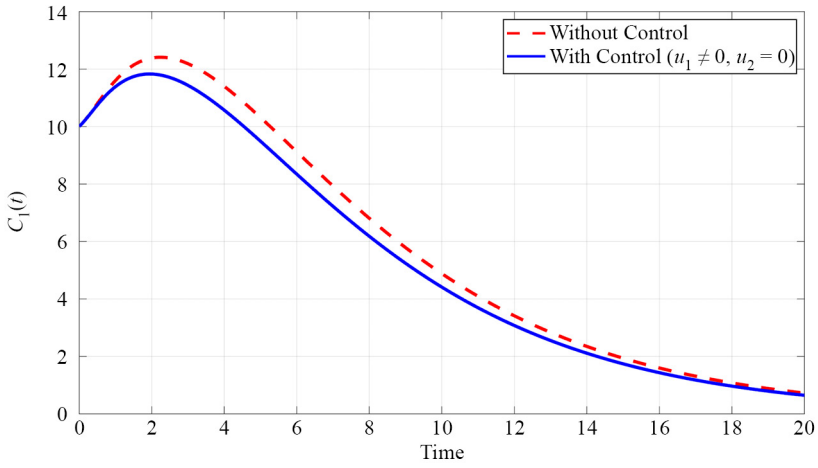

Figure 16. Dynamics of chronic infection from the first strain when only vaccination is implemented

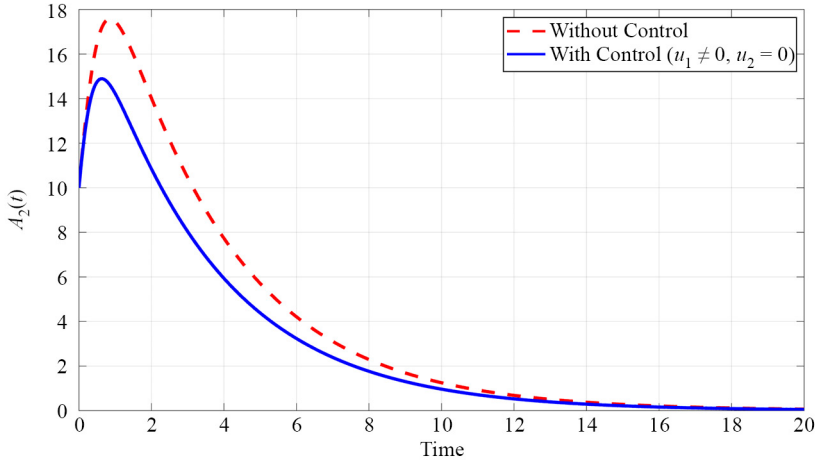

Figure 17. Dynamics of acute infection from the second strain when only vaccination is implemented

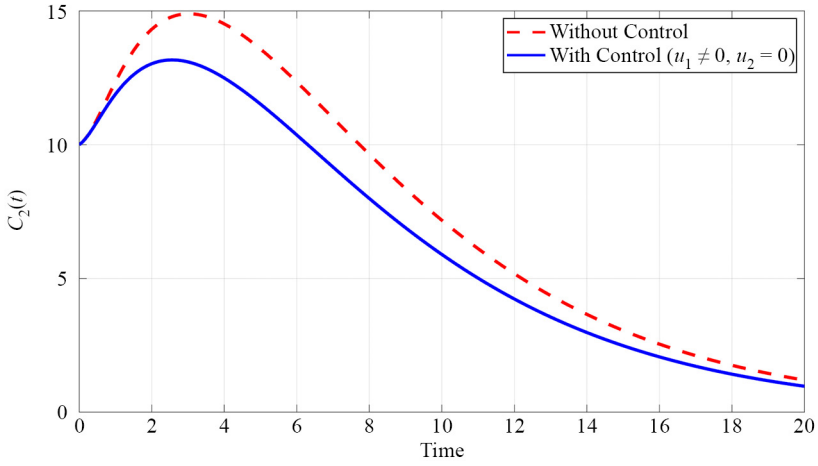

Figure 18. Dynamics of chronic infection under vaccination-only intervention

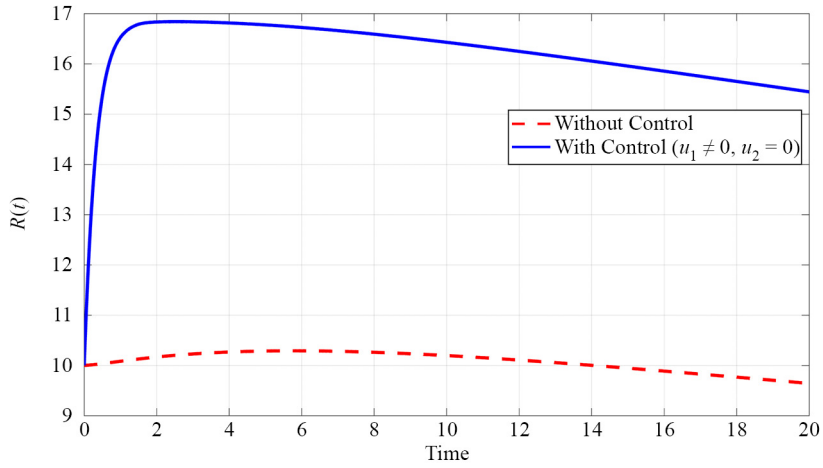

Figure 19. Dynamics of chronic infection under vaccination-only intervention

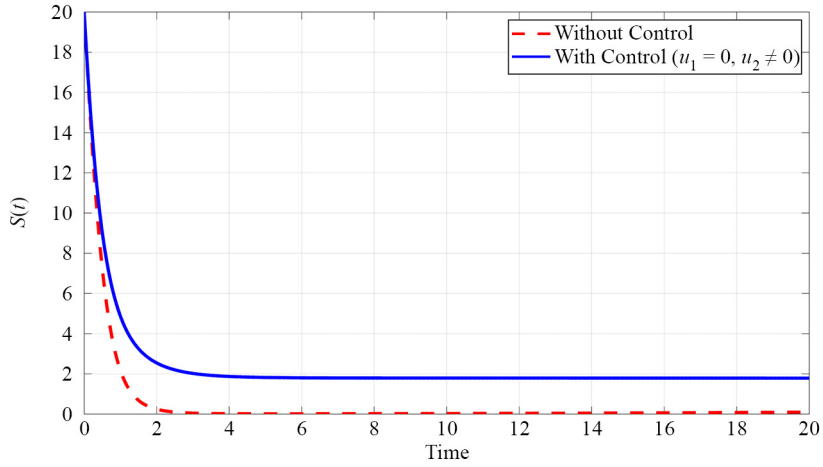

Figure 20. Susceptible population dynamics under treatment-only intervention

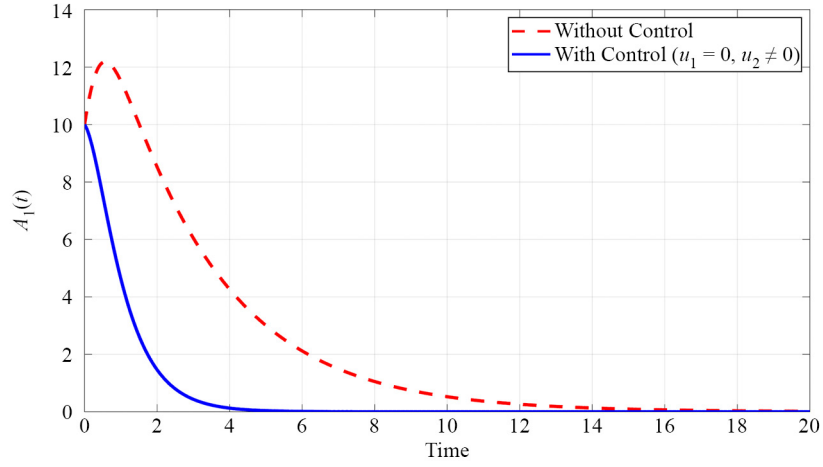

Figure 21. Dynamics of acute infection from the first HBV strain under treatment-only control

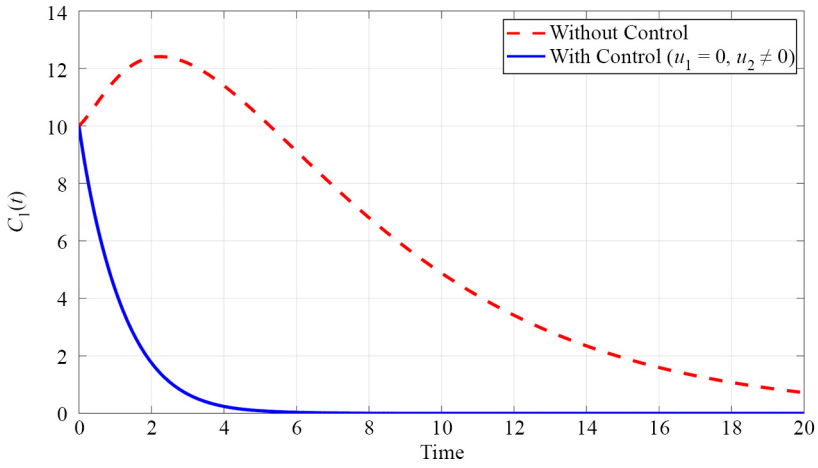

Figure 22. Dynamics of chronic infection from the first HBV strain under treatment-only control

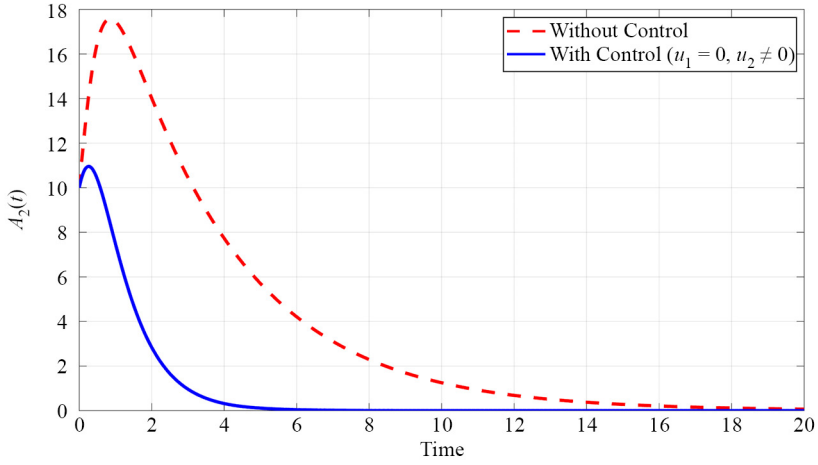

Figure 23. Dynamics of acute infection from the second HBV strain under treatment-only intervention

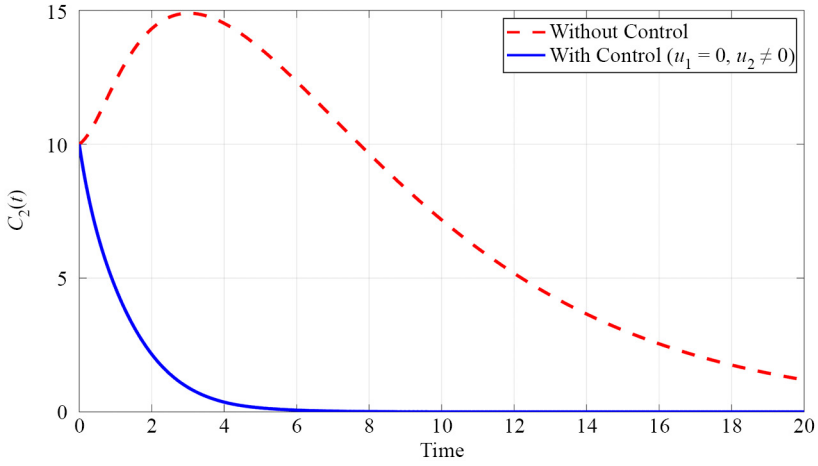

Figure 24. Dynamics of chronic infection from the second HBV strain under treatment-only intervention

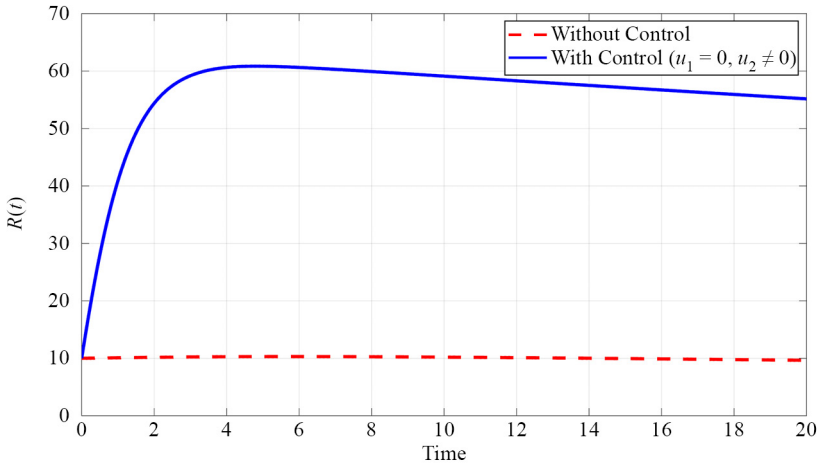

Figure 25. Dynamics of $R(t)$ under treatment-only control intervention

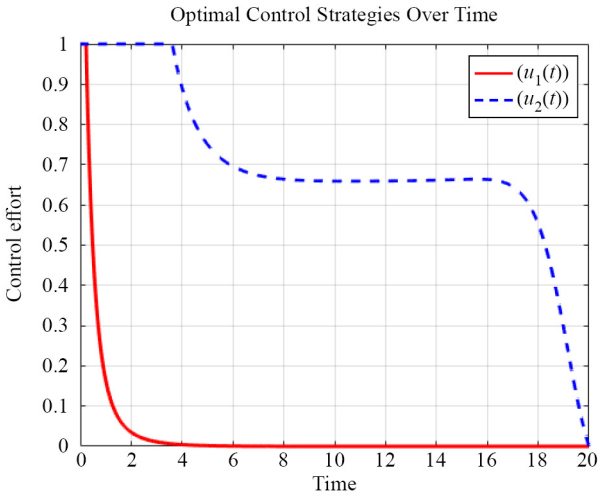

Figure 26. control profile of u_1 and u_2

Following the implementation of two distinct control strategies, a numerical simulation was performed to evaluate their respective effectiveness, with each control strategy activated individually. The coupled state–adjoint system is solved using the forward–backward sweep method. Both state and adjoint equations are integrated using the classical fourth-order Runge–Kutta method with a fixed time step. The final simulation time $T = 20$ was chosen to ensure that the model captures both the transient and long-term behavior of the system, and to allow the assessment of the cumulative impact of the applied control strategies. The initial condtions are $S(0) = 20,\ A_1(0) = 10,\ A_2(0) = 10,\ C_1(0) = 10,\ A_2(0) = 10,\ C_2(0) = 10$ and $R(0) = 10$.

The control variables are updated iteratively at each time point until convergence. Initially, the optimal control model (16) was simulated as shown in Figures 8-13. The implementation of the control strategies demonstrated significant effectiveness in reducing the transmission of all forms of infection. Subsequently, the model was simulated with the exclusive activation of the treatment strategy, corresponding to $u_1 = 0$ and $u_2 \neq 0$ in Figures 20-25.

Subsequently, the simulation was repeated with the vaccination strategy exclusively activated, corresponding to $u_2 = 0$ and $u_1 \neq 0$ in Figures 14-19.

As shown in Figure 26, the optimal control strategies for vaccination ($u_1(t)$) and treatment ($u_2(t)$) exhibit a clear pattern. The vaccination effort, $u_1(t)$, is applied at its maximum level initially and then rapidly decreases, becoming negligible after approximately four time units. In contrast, the treatment control, $u_2(t)$, is also applied at its maximum level at the beginning but is sustained at a high-to-moderate level for a much longer duration. It gradually decreases around time unit 17 and eventually phases out towards the end of the time horizon. This suggests that while an aggressive initial vaccination campaign is crucial, treatment is a more sustainable and essential long-term strategy for effectively managing the disease.

The Efficiency Index (E.I.) of the model was computed using MATLAB. It is calculated using the formula: $E.I. = \left(1 - \frac{A_c}{A_0}\right) \times 100$ where A_0 denotes the cumulative number of liver cirrhosis cases without any control, and A_c refers to the cumulative number under a specific control strategy.

The quantity $A = \int_0^{20} C_1\, dt$ represents the total number of individuals who developed liver cirrhosis. The strategy that yields a higher E.I. is considered more effective in reducing disease transmission. The values of A_0, A_c, and the E.I. for both control strategies are summarized in Table 2 below:

Table 2. Comparison between the two control strategies

Control Strategy	A_0	A_c	E.I.
treatment strategy	117.3926	11.4294	90.26%
vaccination strategy	117.3926	109.0980	7.07%

The simulation results revealed a substantial reduction in the number of cases of liver cirrhosis, which produced a treatment Effectiveness Index (EI) of approximately 90.26 In contrast, the reduction in liver cirrhosis cases was comparatively modest with vaccination, with the IE reaching approximately 7.07%. In general, the treatment strategy shows significantly greater effectiveness in reducing the spread of liver cirrhosis compared to the vaccination strategy.

8.1 *Cost-effectiveness analysis*

The economic feasibility analysis of control strategies plays a crucial role in elucidating their efficiency, as it informs decision-making based on an objective assessment of costs relative to performance. To perform the cost-effectiveness analysis, we employ the Average Cost-Effectiveness Ratio (ACER) and the Incremental Cost-Effectiveness Ratio (ICER). The following formula is used to determine the ACER [55]:

$$ACER = \frac{\text{The total cost (Tc)}}{\text{Total number of infections averted (Ta)}}. \tag{91}$$

The total number of people whose infections were prevented during the intervention period T is determined using:

$$T_a = \int_0^T (A_1^* + C_1^* + A_2^* + C_2^*)dt - \int_0^T (A_1 + C_1 + A_2 + C_2)dt, \tag{92}$$

where A_1^*, C_1^*, A_2^* and C_2^* represent the solutions for the acute and chronic infected classes of the first and second strains with controls, and A_1, C_1, A_2 and C_2 represents the solutions without controls. Cost implemented during the period T is calculated as follows:

$$T_c = \int_0^T \frac{1}{2}(K_5 u_1^2 + K_6 u_2^2)dt. \tag{93}$$

The ICER is calculated by dividing the difference in costs between two feasible interventions by the difference in their effects, and it is represented as[56]:

$$ICER = \frac{\text{Difference in costs produced by strategies i and j}}{\text{Difference in the total number of infections averted in strategies i and j}}. \tag{94}$$

The computed values of total cost, infections averted, AECR, and ICER for each strategy were obtained using MATLAB simulations. The results are summarized in Tables 3 and 4.

Table 3. Analysis of ACER and ICER for Different Strategies

Strategy	Total infections averted T_a	Total cost T_c	ACER	ICER
Vaccine & Treatment	349.54	9,322.3	26.67	26.67
Vaccine	51.148	2,589.8	50.634	50.634
Treatment	342.99	8,114.4	23.658	23.658

Table 4. Comparison of Strategies Based on ICER

Comparison	ICER
Vaccine & Treatment VS Vaccine	22.562
Vaccine & Treatment VS Treatment	184.28

From Table 3, the economic feasibility of three health intervention strategies was assessed: Vaccination alone, treatment alone, and combination of vaccination and treatment, where the strategy that records the lowest ACER value is considered the most efficient and cost-effective [55], and based on the results received, the treatment alone strategy recorded the lowest ACER value of 23.658, indicating that it is the most cost-effective and economically efficient. Regarding the ICER analysis, the results, in addition to what is mentioned in Table 4, supported the above, it was found that the comparison of treatment only without intervention gave the best ICER value of 22.526.

Based on this, it is concluded that the treatment-only strategy is the most cost-effective option, while the vaccination-only strategy is the least economically feasible within this analytical model. While the model identifies theoretically optimal time-dependent vaccination ($u_1(t)$) and treatment ($u_2(t)$) strategies, their real-world implementation may face several challenges, including resource limitations, logistical constraints, population compliance, and vaccine/treatment availability.

The superior cost-effectiveness of treatment is attributed to its direct and immediate effect on reducing infection prevalence, as well as its relatively lower cost per unit of implementation compared to vaccination. This makes treatment particularly advantageous in short-term control efforts or resource-constrained settings.

Although treatment emerged as the more cost-effective intervention in the short term, its long-term sustainability depends on continuous funding, healthcare access, and patient adherence. Preventive strategies such as vaccination may complement treatment efforts by offering more durable protection and reducing long-term healthcare costs.

In practice, public health interventions often require discretized or step-wise implementations rather than continuous time-varying controls. Nevertheless, the results of the model can inform the design of realistic intervention schedules by highlighting critical periods where intensified control efforts are most effective.

9. Conclusions

This study developed a mathematical model to describe the transmission dynamics of the HBV, accounting for two distinct viral strains. The basic reproduction number R_0 was derived using the next-generation matrix method, and a comprehensive stability analysis was conducted. The disease-free equilibrium was shown to be locally asymptotically stable when $R_0 < 1$, while the strain-free equilibrium is stable when $R_{02} > R_{01}$, consistent with the competitive exclusion principle. In contrast, the endemic equilibrium becomes stable when $R_0 > 1$, indicating the potential long-term coexistence or dominance of the more transmissible strain.

In addition, numerical simulations were conducted to evaluate the effectiveness of two optimal control strategies: treatment and vaccination. The results demonstrate that treatment is more effective in reducing infection levels compared to vaccination alone. Cost-effectiveness analysis further supports this conclusion, identifying the treatment-only strategy as the most economically viable intervention. Accordingly, prioritizing treatment may provide the most practical and impactful means of controlling HBV spread, particularly in resource-limited settings.

The proposed framework can be adapted to other viral infections with comparable transmission mechanisms by appropriately redefining the epidemiological parameters and compartments. In particular, the same incidence structure and stability/optimal–control analyses remain valid after replacing HBV-specific flows (e.g., chronic/progression rates and vaccination efficacy) with disease-specific counterparts.

The present model adopts several simplifying assumptions, including constant parameters, a deterministic framework, and homogeneous mixing. It does not account for reinfection, population heterogeneity, or stochastic effects. Future research may aim to enhance the model by incorporating reinfection mechanisms, age-structured or spatially heterogeneous populations, and stochastic perturbations to better reflect the complex nature of HBV transmission in real-world scenarios.

Acknowledgements

The authors gratefully acknowledge Qassim University, represented by the Deanship of Graduate Studies and Scientific Research, for the financial support for this research under the number (QU-J-PG-2-2025-55250) during the academic year 1446 AH/2024 AD.

Conflict of interest

The authors declare no competing financial interest.

References

[1] Libbus MK, Phillips LM. Public health management of perinatal hepatitis B virus. *Public Health Nursing*. 2009; 26(4): 353-361.

[2] Mann J, Roberts M. Modelling the epidemiology of hepatitis B in New Zealand. *Journal of Theoretical Biology*. 2011; 269(1): 266-272.

[3] Neuveut C, Wei Y, Buendia MA. Mechanisms of HBV-related hepatocarcinogenesis. *Journal of Hepatology*. 2010; 52(4): 594-604.
[4] World Health Organization. *WHO Sounds the Alarm: Viral Hepatitis Infections Claiming 3,500 Lives Each Day*. PAHO News; 2024. Available from: https://www.paho.org/en/news/10-4-2024-who-sounds-alarm-viral-hepatitis-infections-claiming-3500.
[5] World Health Organization. *Hepatitis B Fact Sheet*. World Health Organization; 2024. Available from: https://www.who.int/news-room/fact-sheets/detail/hepatitis-b.
[6] Centers for Disease Control and Prevention. *Hepatitis B FAQs for the Public*. Centers for Disease Control and Prevention; 2024. Available from: https://www.cdc.gov/hepatitis-b/about/index.html.
[7] Centers for Disease Control and Prevention. *National Progress Report on Hepatitis B*. Centers for Disease Control and Prevention; 2024. Available from: https://www.cdc.gov/hepatitis/statistics/2024progressreport.
[8] Wang J, Pang J, Liu X. Modelling diseases with relapse and nonlinear incidence of infection: a multi-group epidemic model. *Journal of Biological Dynamics*. 2014; 8(1): 99-116.
[9] Wang J, Zhang R, Kuniya T. The stability analysis of an SVEIR model with continuous age-structure in the exposed and infectious classes. *Journal of Biological Dynamics*. 2015; 9(1): 73-101.
[10] Zaman G, Kang YH, Jung IH. Stability analysis and optimal vaccination of an SIR epidemic model. *BioSystems*. 2008; 93(3): 240-249.
[11] Zaman G, Kang YH, Jung IH. Optimal treatment of an SIR epidemic model with time delay. *BioSystems*. 2009; 98(1): 43-50.
[12] Ahmed M, Jawad S, Das D, Boulaaras S, Osman M. Impact of dust storms on plant biomass: Model structure and dynamic study. *Alexandria Engineering Journal*. 2025; 126: 605-622.
[13] Zouari F. Neural network based adaptive backstepping dynamic surface control of drug dosage regimens in cancer treatment. *Neurocomputing*. 2019; 366: 248-263.
[14] Rigatos G, Abbaszadeh M, Siano P, Al-Numay M, Zouari F. A nonlinear optimal control approach for bacterial infections under antibiotics resistance. *Journal of Systems Science and Complexity*. 2024; 37(6): 2293-2317.
[15] Belay MA, Abonyo OJ, Theuri DM. Mathematical model of hepatitis B disease with optimal control and cost-effectiveness analysis. *Computational and Mathematical Methods in Medicine*. 2023; 2023(1): 5215494.
[16] Shoaib M, Tabassum R, Raja MAZ, Nisar KS. Bio-inspired algorithm integrated with sequential quadratic programming to analyze the dynamics of hepatitis B virus. *Beni-Suef University Journal of Basic and Applied Sciences*. 2024; 13(1): 71.
[17] Ciupe SM, Dahari H, Ploss A. Mathematical models of early hepatitis B virus dynamics in humanized mice. *Bulletin of Mathematical Biology*. 2024; 86(5): 53.
[18] Chen-Charpentier B. A model of hepatitis B viral dynamics with delays. *AppliedMath*. 2024; 4(1): 182-196.
[19] Xue T, Zhang L, Fan X. Dynamic modeling and analysis of Hepatitis B epidemic with general incidence. *Mathematical Biosciences and Engineering*. 2023; 20: 10883-10908.
[20] Xu C, Wang Y, Cheng K, Yang X, Wang X, Guo S, et al. A mathematical model to study the potential hepatitis B virus infections and effects of vaccination strategies in China. *Vaccines*. 2023; 11(10): 1530.
[21] Faniran TS, Adewole MO, Ahmad H, Abdullah FA. Dynamics of tuberculosis in HIV-HCV co-infected cases. *International Journal of Biomathematics*. 2023; 16(03): 2250091.
[22] Khan T, Rihan FA, Ahmad H. Modelling the dynamics of acute and chronic hepatitis B with optimal control. *Scientific Reports*. 2023; 13(1): 14980.
[23] Seyoum Desta B, Koya PR. Modified model and stability analysis of the spread of hepatitis B virus disease. *American Journal of Applied Mathematics*. 2019; (7): 13-20.
[24] Kadelka S, M Ciupe S. Mathematical investigation of HBeAg seroclearance. *Mathematical Biosciences and Engineering*. 2019; 16(6): 7616-7658.
[25] Titus IC, Edmund OE, Godwin CEM. Mathematical model of the dynamics of hepatitis B virus (HBV) infection with controls. *International Journal of Trend in Scientific Research and Development*. 2018; 2(5): 1654-1677.
[26] Khan T, Zaman G, Chohan MI. The transmission dynamic and optimal control of acute and chronic hepatitis B. *Journal of Biological Dynamics*. 2017; 11(1): 172-189.
[27] Attaullah, Boulaaras S, Jan AU, Hassan T, Radwan T. Mathematical modeling and computational analysis of hepatitis B virus transmission using the higher-order Galerkin scheme. *Nonlinear Engineering*. 2024; 13(1): 20240048.

[28] Gul N, Bilal R, Algehyne EA, Alshehri MG, Khan MA, Chu YM, et al. The dynamics of fractional order hepatitis B virus model with asymptomatic carriers. *Alexandria Engineering Journal*. 2021; 60(4): 3945-3955.
[29] Din A, Li Y, Liu Q. Viral dynamics and control of hepatitis B virus (HBV) using an epidemic model, Alexandria Eng. *Alexandria Engineering Journal*. 2020; 59(2): 667-679.
[30] Zhao S, Xu Z, Lu Y. A mathematical model of hepatitis B virus transmission and its application for vaccination strategy in China. *International Journal of Epidemiology*. 2000; 29(4): 744-752.
[31] Kamyad AV, Akbari R, Heydari AA, Heydari A. Mathematical modeling of transmission dynamics and optimal control of vaccination and treatment for hepatitis B virus. *Computational and Mathematical Methods in Medicine*. 2014; 2014(1): 475451.
[32] Onyango NO. Multiple endemic solutions in an epidemic hepatitis B model without vertical transmission. *Applied Mathematics*. 2014; 5: 2518-2529.
[33] Alrabaiah H, Safi MA, DarAssi MH, Al-Hdaibat B, Ullah S, Khan MA, et al. Optimal control analysis of hepatitis B virus with treatment and vaccination. *Results in Physics*. 2020; 19: 103599.
[34] Gaff H, Schaefer E. Optimal control applied to vaccination and treatment strategies for various epidemiological models. *Mathematical Biosciences and Engineering*. 2009; 6(3): 469-492.
[35] Igoe M, Casagrandi R, Gatto M, Hoover CM, Mari L, Ngonghala CN, et al. Reframing optimal control problems for infectious disease management in low-income countries. *Bulletin of Mathematical Biology*. 2023; 85(4): 31.
[36] Kumar A, Srivastava PK, Dong Y, Takeuchi Y. Optimal control of infectious disease: Information-induced vaccination and limited treatment. *Physica A: Statistical Mechanics and Its Applications*. 2020; 542: 123196.
[37] Zhang J, Zhang S. Application and optimal control for an HBV model with vaccination and treatment. *Discrete Dynamics in Nature and Society*. 2018; 2018(1): 2076983.
[38] Khan T, Rihan FA, Ibrahim M, Li S, Alamri AM, AlQahtani SA. Modeling different infectious phases of hepatitis B with generalized saturated incidence: An analysis and control. *Mathematical Biosciences and Engineering*. 2024; 21(4): 5207-5226.
[39] Khan T, Ullah R, Zaman G. Hepatitis B virus transmission via epidemic model. In: *Advances in Epidemiological Modeling and Control of Viruses*. Elsevier; 2023. p.29-54.
[40] Khan A, Zarin R, Hussain G, Usman AH, Humphries UW, Gomez-Aguilar J. Modeling and sensitivity analysis of HBV epidemic model with convex incidence rate. *Results in Physics*. 2021; 22: 103836.
[41] Brauer F, Castillo-Chavez C. *Mathematical Models in Population Biology and Epidemiology, vol. 2.* Springer; 2012.
[42] Diekmann O, Heesterbeek JAP. *Mathematical Epidemiology of Infectious Diseases: Model Building, Analysis and Interpretation, vol. 5*. John Wiley & Sons; 2000.
[43] Chen D, Xu Z. Global dynamics of a delayed diffusive two-strain disease model. *Differential Equations and Applications*. 2016; 8(1): 99-122.
[44] Bentaleb D, Amine S. Lyapunov function and global stability for a two-strain SEIR model with bilinear and non-monotone incidence. *International Journal of Biomathematics*. 2019; 12(02): 1950021.
[45] Baba IA, Hincal E. Global stability analysis of two-strain epidemic model with bilinear and non-monotone incidence rates. *The European Physical Journal Plus*. 2017; 132: 1-10.
[46] Meskaf A, Khyar O, Danane J, Allali K. Global stability analysis of a two-strain epidemic model with non-monotone incidence rates. *Chaos, Solitons & Fractals*. 2020; 133: 109647.
[47] Khyar O, Allali K. Global dynamics of a multi-strain SEIR epidemic model with general incidence rates: application to COVID-19 pandemic. *Nonlinear Dynamics*. 2020; 102(1): 489-509.
[48] Saha P, Mondal B, Ghosh U. Global dynamics and optimal control of a two-strain epidemic model with non-monotone incidence and saturated treatment. *Iranian Journal of Science*. 2023; 47(5): 1575-1591.
[49] Hu Y, Wang H, Jiang S. Analysis and optimal control of a two-strain SEIR epidemic model with saturated treatment rate. *Mathematics*. 2024; 12(19): 3026.
[50] Van den Driessche P, Watmough J. Reproduction numbers and sub-threshold endemic equilibria for compartmental models of disease transmission. *Mathematical Biosciences*. 2002; 180(1-2): 29-48.
[51] Castillo-Chavez C, Feng Z, Huang W. On the computation of R_0 and its role on global stability. In: Castillo-Chavez C, Blower S, van den Driessche P, Kirschner D, Yakubu AA. (eds.) *Mathematical Approaches for Emerging and Reemerging Infectious Diseases: An Introduction*. Berlin: Springer; 2002. p.229-250.
[52] Castillo-Chavez C, Song B. Dynamical models of tuberculosis and their applications. *Mathematical Biosciences & Engineering*. 2004; 1(2): 361-404.

[53] Zaman G, Kang YH, Jung IH. Optimal treatment of an SIR epidemic model with time delay. *BioSystems*. 2009; 98(1): 43-50.

[54] Osman S, Otoo D, Sebil C. Analysis of listeriosis transmission dynamics with optimal control. *Applied Mathematics*. 2020; 11(7): 712-737.

[55] Memarbashi R, Mahmoudi SM. A dynamic model for the COVID-19 with direct and indirect transmission pathways. *Mathematical Methods in the Applied Sciences*. 2021; 44(7): 5873-5887.

[56] Fatmawati, Dyah Purwati U, Riyudha F, Tasman H. Optimal control of a discrete age-structured model for tuberculosis transmission. *Heliyon*. 2020; 6(1): 2405-8440.